

An Atlas of Stationary Bow Shock Arcs in the Orion Nebula

WILLIAM J. HENNEY, LUIS A. GUTIÉRREZ-SOTO, JORGE A. TARANGO-YONG, NAHIELY FLORES-FAJARDO¹

¹*Instituto de Radioastronomía y Astrofísica, Universidad Nacional Autónoma de México, Apartado Postal 3-72, 58090 Morelia, Michoacán, Mexico;
w.henney@crya.unam.mx, l.gutierrez@crya.unam.mx, j.tarango@crya.unam.mx*

Abstract

We present a complete catalog of all the stationary emission line arcs (LL objects and proplyd bowshocks) found in archival HST imaging of the Orion Nebula. The total number of objects detected is 73, of which 20 have not previously been reported in the literature. We classify the shapes of emission line arcs by fitting conic sections to the inner and outer shell boundaries and calculate the background corrected H alpha surface brightness of each object. We find significant differences in the shell shapes between the objects closest to the ionizing stars and those farther away. The closer group, which all represent proplyd interactions with the hypersonic stellar wind, have relatively closed shapes, while the farther group, which are due to interactions with the transonic ionized champagne flow in the nebula, are more open and hyperbolic. Although some of the latter group are also known proplyds, many are not, and the largest and brightest arcs tend to be associated with particularly luminous young stars, suggesting that the intrinsic T Tauri disk wind may play a role. The orientations of the arcs, together with the stagnation pressures estimated from the surface brightness, allow the internal velocity field of the H II region to be probed. We find that approximately radial flows from the core of the nebula dominate over disordered, turbulent flows.

1. INTRODUCTION

2. OBSERVATIONS

We have attempted to identify and characterize all stationary emission-line arcs in archival HST imaging observations of the Orion Nebula, obtained with the WFPC2 and ACS cameras, as summarized in Table 1. The primary dataset that we have used is the 26-orbit Cycle 12 program GO 9825 (Bally et al. 2006). This program covered a significant fraction of the entire nebula with the ACS/WFC camera in the filter F658N, which transmits the lines H α λ 6563 and [N II] λ 6584. The combination of good spatial resolution and signal-to-noise of this dataset makes it ideal for detecting the faint arcs against the varying nebular background. For regions in the outskirts of the nebula that are outside of the GO 9825 fields, we used observations with the same camera and filter from the 104-orbit Cycle 13 program GO 10246 (*HST* Treasury Program on the Orion Nebula Cluster, Robberto et al. 2013). In addition, we have used images from the same program obtained with the F656N filter of the WFPC2 camera. The resolution¹ and signal-to-noise of these observations is significantly worse than the ACS images, but they have the important advantage that the WFPC2 F656N filter is considerably narrower (≈ 5 Å) than the ACS F658N filter (≈ 15 Å) and suffers relatively little contamination from [N II]. For regions in the

core of the nebula, we have used older WFPC2 images from programs GTO 5085 (O'Dell & Wong 1996) and GO 5469 (Bally et al. 1998). These offer two advantages for the study of the bowshocks closest to the Trapezium OB stars: shorter exposure times mean that the bright stars are less saturated, and images were obtained in a much wider range of emission line filters. Finally, for regions in the core and southern outskirts we have used the Cycle 21 program GO 13419 (Bally & Reipurth 2018) to check for high proper motions over the 21 year baseline 1994–2015, which would rule out any given filament being a stationary arc.

For each arc, we trace by eye the inner and outer boundaries of the emission line shell and mark along each edge using “point” regions with the SAOimage ds9 program², and in addition mark the position of the central star or proplyd (hereafter, central source). These are shown in Figure 2 as yellow crosses, yellow pluses and blue circle for the outer edge, inner edge, and proplyd, respectively, for an illustrative case. We then fit circular arcs to the points, determining the center and radius of curvature R_c of each edge. The fits are carried out with the aid of the python library lmfit³, which implements a Levenberg–Marquardt curve-fitting algorithm. The initial parameter estimates for each fit are obtained as follows. First, the sky coordinates (α_i, δ_i) of the edge points are converted to polar coordinates with respect to the central

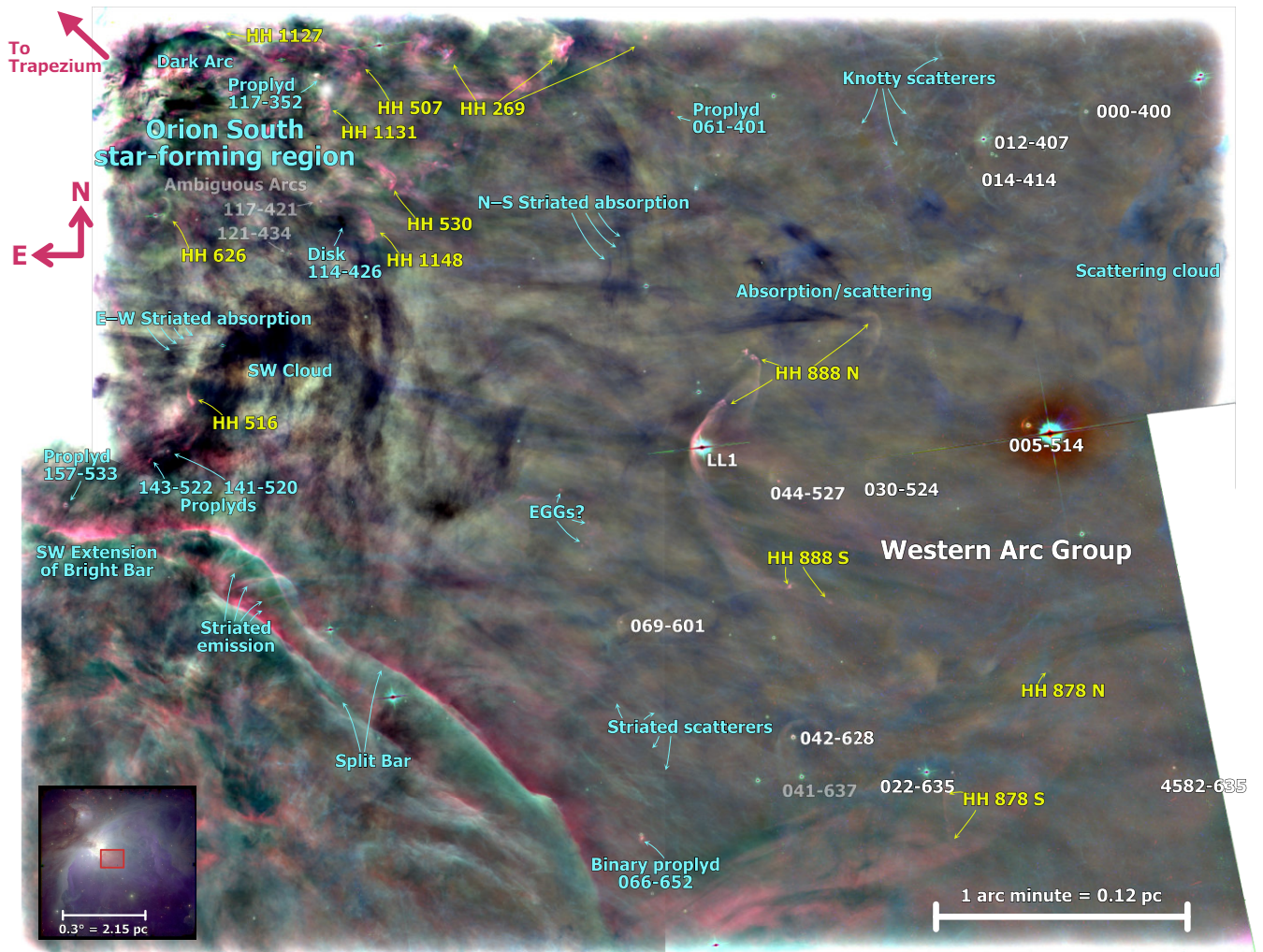
¹ The point spread function is very similar for the two cameras (FWHM $\approx 0.082''$ at H α), but it is not well-sampled by the larger 0.1'' pixels of the three WFC chips of WFPC2.

² <http://ds9.si.edu>

³ <https://pypi.python.org/pypi/lmfit/>

Table 1. Archival *HST* imaging datasets used in this study

| Year | Instrument | Program(s) | Field size | Pixel size | Filters |
|--------|------------|-------------------|------------|------------|--|
| 1994–5 | WFPC2/WFC | GTO 5085, GO 5469 | 5' × 10' | 0.1" | F656N, F658N, F502N, F547M |
| 1994–5 | WFPC2/PC | GO 5469 | 1' × 2' | 0.045" | F656N, F658N, F502N, F673N, F631N, F547M |
| 2004 | ACS/WFC | GO 10057 | 1' × 1' | 0.045" | FR505N |
| 2004 | ACS/WFC | GO 9825 | 20' × 20' | 0.05" | F658N |
| 2004–5 | ACS/WFC | GO 10246 | 25' × 30' | 0.05" | F658N, F435W, F555W, F775W, F850LP |
| 2004–5 | WFPC2/WFC | GO 10246 | 25' × 30' | 0.1" | F656N |
| 2015 | WFC3/UVIS | GO 13419 | 8' × 12' | 0.05" | F656N, F225W, F336W, F280N, F373N |

**Figure 1.** A particularly rich region of the Orion Nebula, centered on LL Ori, the largest member of the Western group of stationary arcs.

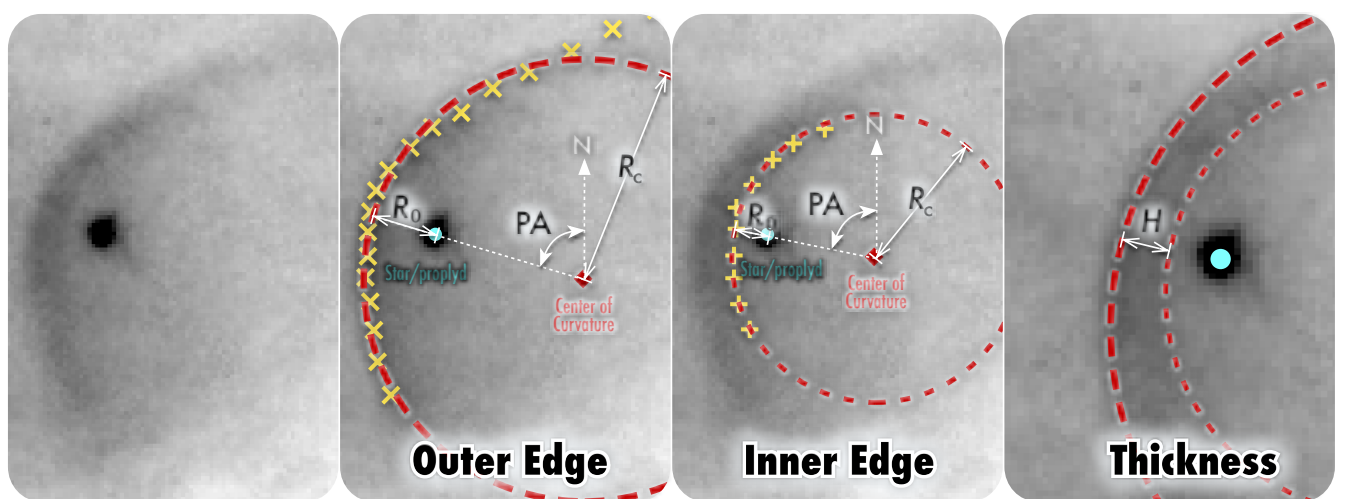


Figure 2. Methodology for determining geometric parameters of the arcs.

source: (r_i, θ_i) , where θ is a position angle (degrees counter-clockwise from north). After sorting the edge points in θ , the smallest value of r_i , together with its immediate neighbors to either side are used to define a parabola in polar coordinates, the root of whose derivative gives the point (r_0, θ_0) of closest approach of the arc's edge to the central source.⁴ The initial estimate for the position of the center of curvature is taken to be the same distance from the central source as the point of closest approach, but on the “other side” of the source: that is at polar coordinates $(r_0, \theta_0 + 180^\circ)$. The sky coordinates of this center of curvature (α_c, δ_c) are the only two formal parameters of the circle fit since the circle radius is estimated on the fly as the mean distance $\langle R_c \rangle$ from (α_c, δ_c) to the individual edge points (α_i, δ_i) . Only those edge points satisfying the condition $|\theta_j - \theta_0| \leq 90^\circ$ are used in the fit.

3. CATALOG

3.1. LV knot group

The LV knot group is a six proplyds set that were discovered by Laques & Vidal (1979), located very close to the Trapezium and show an isotropic distribution. There is a binary system in this group. The emission arcs were identified after. In general, these arcs are very weak, which makes it difficult to trace the edges of the shells.

158-323 (LV5). This was previously catalogued as a round head with tail by O’Dell & Wong (1996). After, it was reported as a proplyd and binary system by (Ricci et al. 2008). An emission arc wraps around this proplyd.

161-324 (LV4). This small and bright proplyd was previously catalogued by O’Dell & Wong (1996); Ricci et al. (2008). The proplyd is surrounded by a faint but well-defined emission arc. It is located about $4.0''$ to the southeast of 158-323.

163-317 (LV3). This proplyd previously catalogued by O’Dell & Wong (1996); Ricci et al. (2008) is surrounded by a faint and small emission arc.

166-316. (LV2b) This was reported as a circularly symmetric source by O’Dell & Wong (1996). Later, this source was catalogued as a proplyd by Ricci et al. (2008).

167-317 (LV2). This bright proplyd was previously catalogued by O’Dell & Wen (1994); Ricci et al. (2008). It exhibits a long tail. An obvious emission arc (Bally et al. 2000) wraps around the proplyd. Bally et al. (2000) describe a compact microjet emerging from this proplyd.

168-328. This small proplyd was previously reported by O’Dell & Wen (1994) and Ricci et al. (2008). An emission arc

is associated with this proplyd. The arc is much fainter than the proplyd. This object is located about $2.1''$ to the southwest of LV1.

168-326 (LV1). This is a previously reported proplyd designated 168-326S (O’Dell & Wen 1994). This proplyd was classified as a binary system by Ricci et al. (2008). An arc emission with a complex morphology is surrounded this proplyd.

3.2. Southeast group

The southeast group is located to the inside of the Orion Nebula. The central sources of their members are proplyds and their LL arcs associated have not been previously reported in the literature. Their diffuse shells are very thin.

169-338. This is a small and faint previously reported proplyd (O’Dell & Wen 1994; Ricci et al. 2008) with a well defined tail. The emission arc associated to this proplyd is very faint and clumpy but well-defined.

177-341 (HST 1). This very large proplyd with a long tail was previously catalogued by O’Dell & Wen (1994); Ricci et al. (2008). There is probably a jet that emerges from the proplyd (Bally et al. 2000). We identified a well-defined but faint emission arc associated with this proplyd.

180-331. This was first catalogued as a star by O’Dell & Wong (1996). Later, this was reported as a proplyd and a binary system by Ricci et al. (2008). The proplyd is surrounded by a highly asymmetric emission arc.

189-329. The central source was first classified as star by O’Dell & Wong (1996) and later as a proplyd by Ricci et al. (2008). This object is a very faint proplyd associated with a very diffuse shell. The northern bow wing is much more extended than the southern wing. The fact that the shell is so large and diffuse, may be an indication that it is not related to the proplyd, although the fact that a small cavity is seen around the proplyd suggests that some degree of physical interaction is indeed occurring.

3.3. North group

The north group is located inside of the orion Nebula.

142-301. The central source was first catalogued as cusp with tail (O’Dell & Wong 1996) and later as proplyd (Bally et al. 2000; Ricci et al. 2008). This large proplyd has one of the longest tails ($4''$) of any proplyd and does not have a hemispherical head. Instead, the ionization front appears to trace the disk surface, which is inclined with respect to the tail by about 55° . The proplyd tail points away from θ^1 Ori A instead of θ^1 Ori C and exhibits some bends and wiggles (Bally et al. 2000). This proplyd is surrounded by a very faint emission arc. Rather than showing continuous curvature, the emission arc appears to comprise two straight edges, which meet at a point south-east of the proplyd, with the shell being thicker on the southern side.

⁴ This technique will fail if the closest edge point does not have a neighbor to one side, that is, if it is at one end of the traced edge. Such a situation is occasionally found when the observed arc is very asymmetric. In this case a parabola is fitted to all of the edge points (r_i, θ_i) in order to determine (r_0, θ_0) .

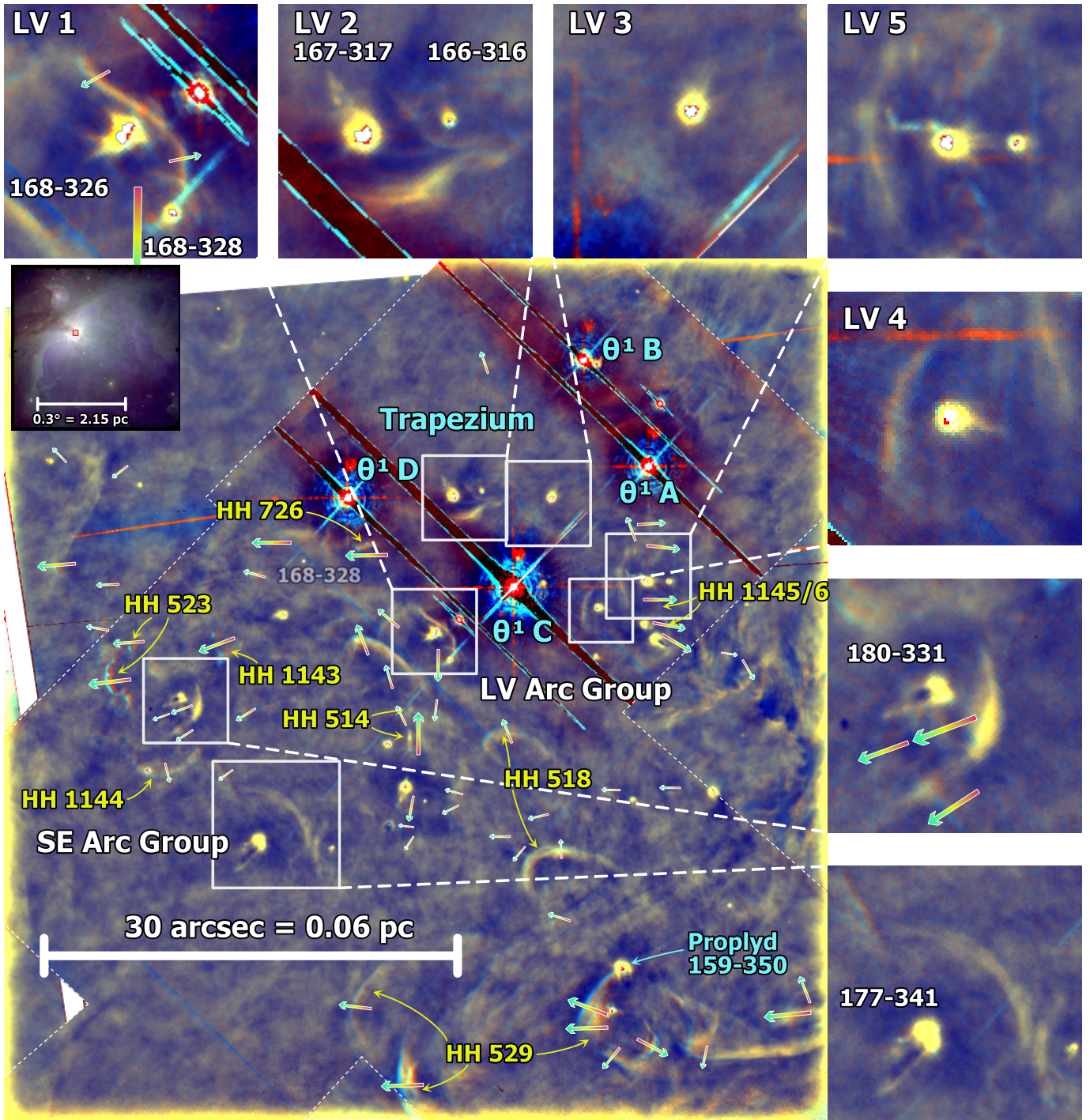


Figure 3. Multi-epoch image of the central core of the Orion Nebula, showing the Trapezium group and part of the Southeast group of arcs. The first epoch is shown in red, the second epoch in green, and the difference in blue. As a result, bright stationary features appear as yellow, whereas features with high proper motion appear blue on the leading edge and red on the trailing edge. For the majority of the field the two epochs are 1995-03 and 2004-01 in [O III] filters, whereas for the regions outside the thin dashed lines the two epochs are 2005-04 and 2015-01 in H α filters. In all cases, the images were high-pass filtered with a kernel width of 1 arcsec.

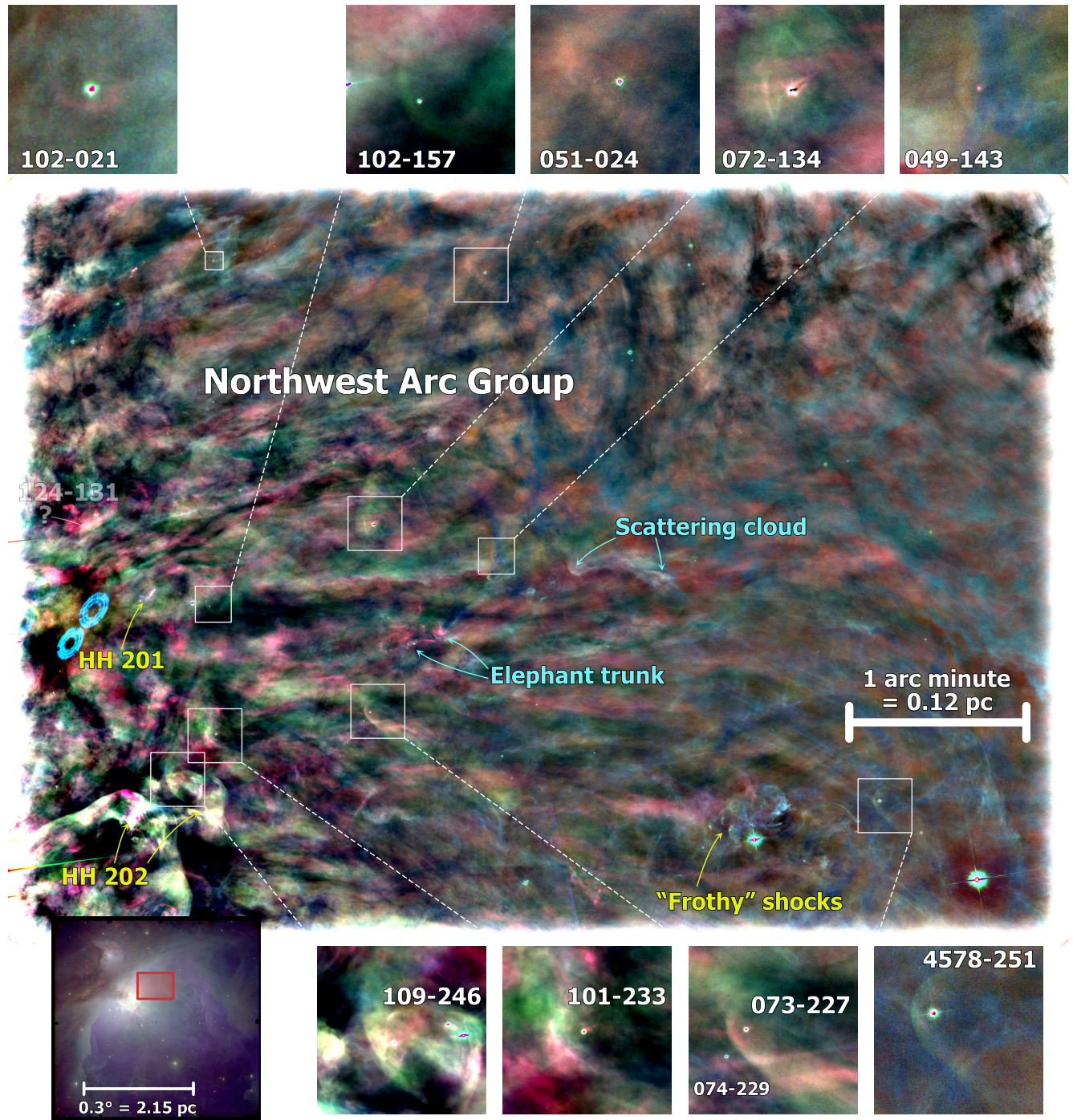


Figure 4. As Figure 1 but for the Northwest group of arcs.

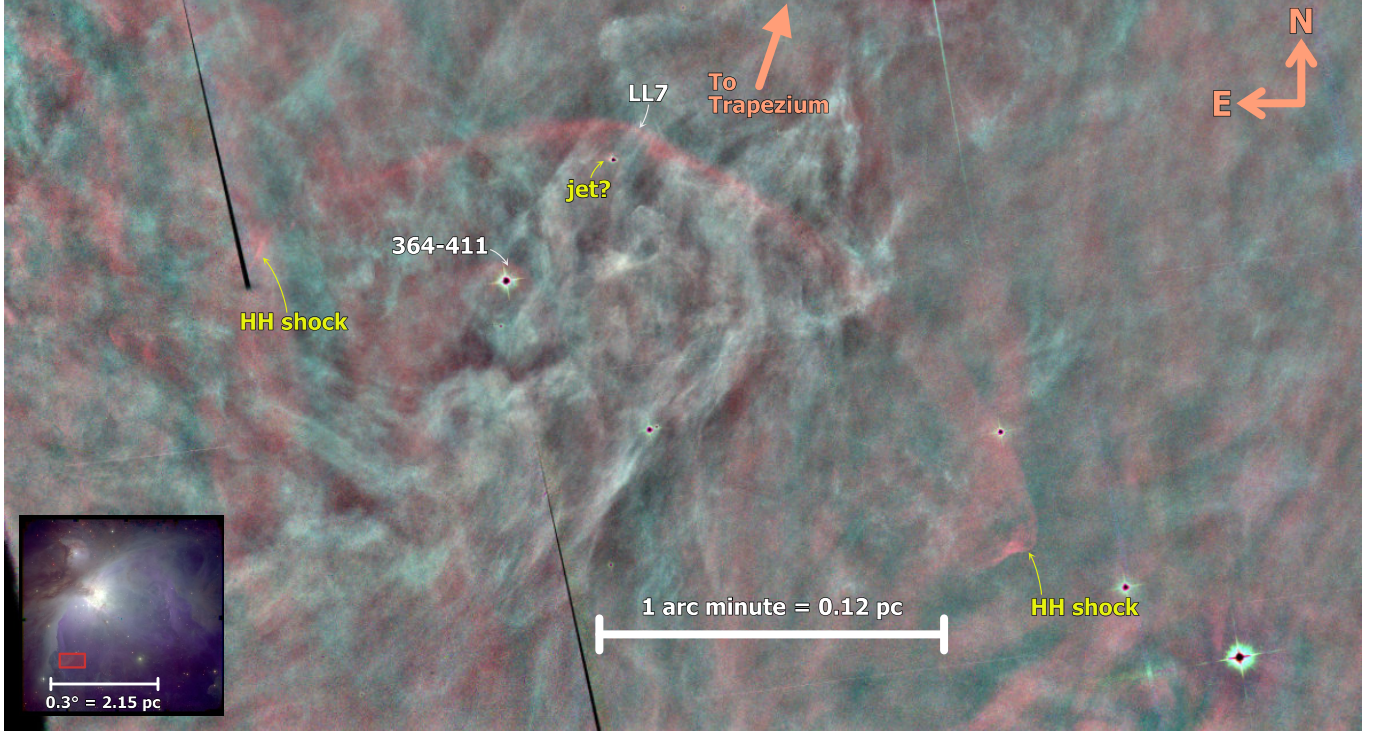


Figure 5. As Figure 1 but for the region around LL7 in the far south of the Orion Nebula.

Table 2. Shell geometric parameters of lv knots

| Object | RA | Dec | D | PA | R_{out} | R_{in} | Π_{out} | Π_{in} | Λ_{out} | Λ_{in} | h | PA_{out} | PA_{in} | Star ID |
|---------|-------------|-------------|------|-------|------------------|-----------------|--------------------|-------------------|------------------------|-----------------------|------|--------------------------|-------------------------|-----------|
| 158-323 | 05:35:15.83 | -05:23:22.5 | 8.34 | 90.1 | 1.85 | 1.64 | 1.89 | 2.12 | | | 0.21 | 114.8 | 120.0 | ACS 4260 |
| 161-324 | 05:35:16.06 | -05:23:24.3 | 5.29 | 70.1 | 1.16 | 0.90 | 2.80 | 3.27 | 2.19 | | 0.26 | 70.7 | 76.6 | ACS 4383 |
| 163-317 | 05:35:16.28 | -05:23:16.6 | 6.11 | 164.8 | 2.32 | 1.93 | 1.92 | 1.12 | 1.29 | | 0.40 | 148.6 | 145.5 | ACS 4427 |
| 166-316 | 05:35:16.61 | -05:23:16.2 | 7.15 | 207.0 | 0.69 | 0.41 | 1.51 | 1.71 | | | 0.28 | 181.4 | 160.5 | ACS 4470 |
| 167-317 | 05:35:16.74 | -05:23:16.5 | 7.97 | 220.9 | 1.96 | 1.25 | 2.29 | | 1.65 | | 0.71 | 178.1 | 165.4 | RSS 10079 |
| 168-328 | 05:35:16.76 | -05:23:28.1 | 7.79 | 315.2 | 1.06 | 0.79 | 1.52 | 1.70 | | | 0.27 | 345.3 | 353.0 | ACS 4552 |
| 168-326 | 05:35:16.84 | -05:23:26.3 | 7.71 | 299.5 | 0.95 | 0.74 | 41.37 | 7.58 | 3.07 | | 0.20 | 314.5 | 328.1 | ACS 4537 |

Table 3. Shell geometric parameters of southeast group

| Object | RA | Dec | D | PA | R_{out} | R_{in} | Π_{out} | Π_{in} | Λ_{out} | Λ_{in} | h | PA_{out} | PA_{in} | Star ID |
|---------|-------------|-------------|-------|-------|------------------|-----------------|--------------------|-------------------|------------------------|-----------------------|------|--------------------------|-------------------------|----------|
| 169-338 | 05:35:16.88 | -05:23:38.0 | 17.14 | 334.7 | 1.03 | 0.68 | | 1.84 | | | 0.35 | 345.9 | 6.4 | ACS 4546 |
| 177-341 | 05:35:17.67 | -05:23:41.0 | 26.54 | 314.0 | 3.81 | 3.06 | 1.12 | 1.14 | | | 0.75 | 317.0 | 293.7 | ACS 4799 |
| 180-331 | 05:35:18.03 | -05:23:30.8 | 25.91 | 288.7 | 1.44 | 1.11 | 1.53 | 1.99 | 1.34 | 1.72 | 0.33 | 280.8 | 282.0 | ACS 4929 |
| 189-329 | 05:35:18.87 | -05:23:28.9 | 37.56 | 279.7 | 1.40 | 0.54 | 2.49 | 1.23 | 3.03 | 1.30 | 0.86 | 296.4 | 264.0 | ACS 5138 |

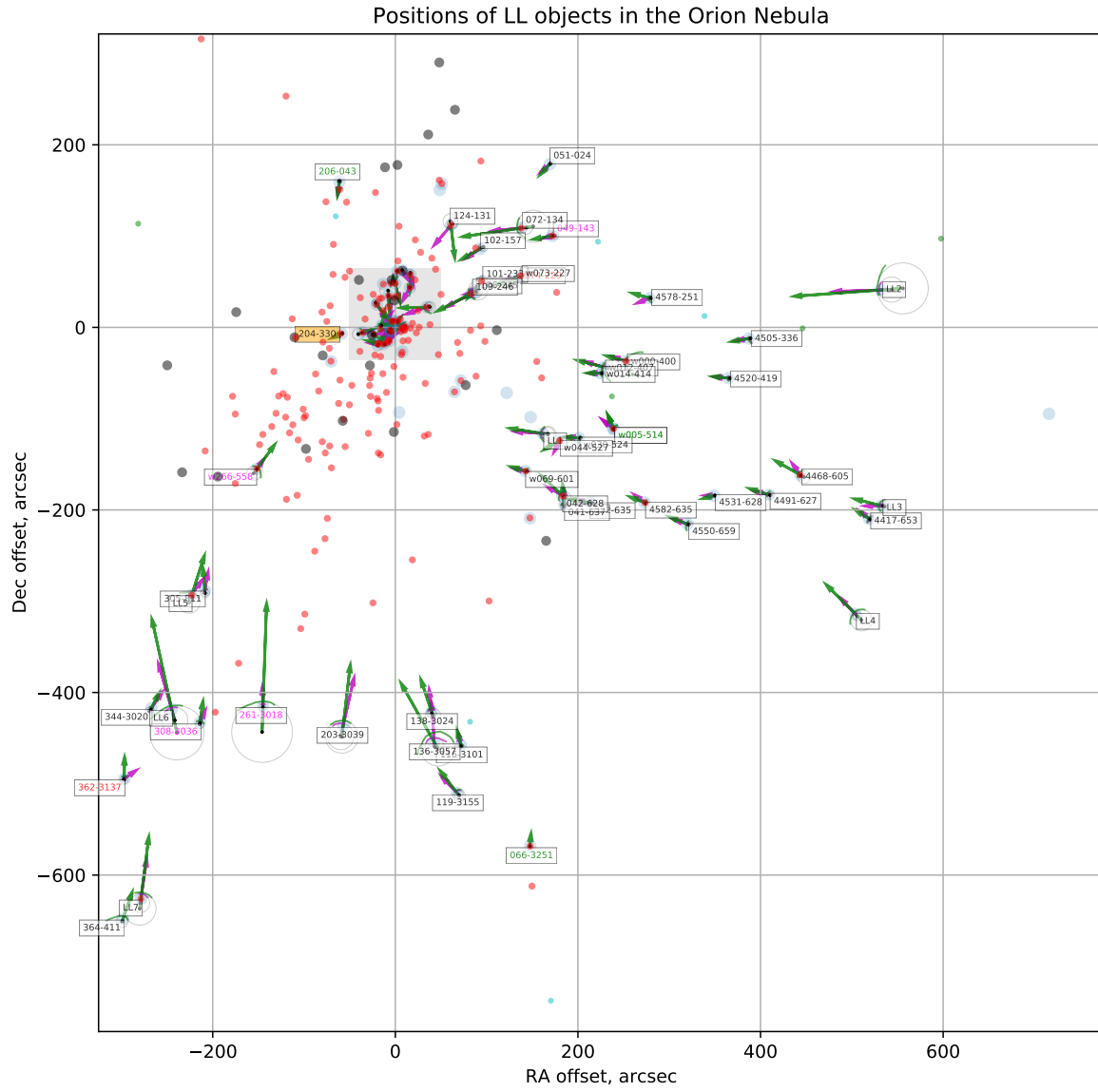


Figure 6. Position of bow shock arcs.

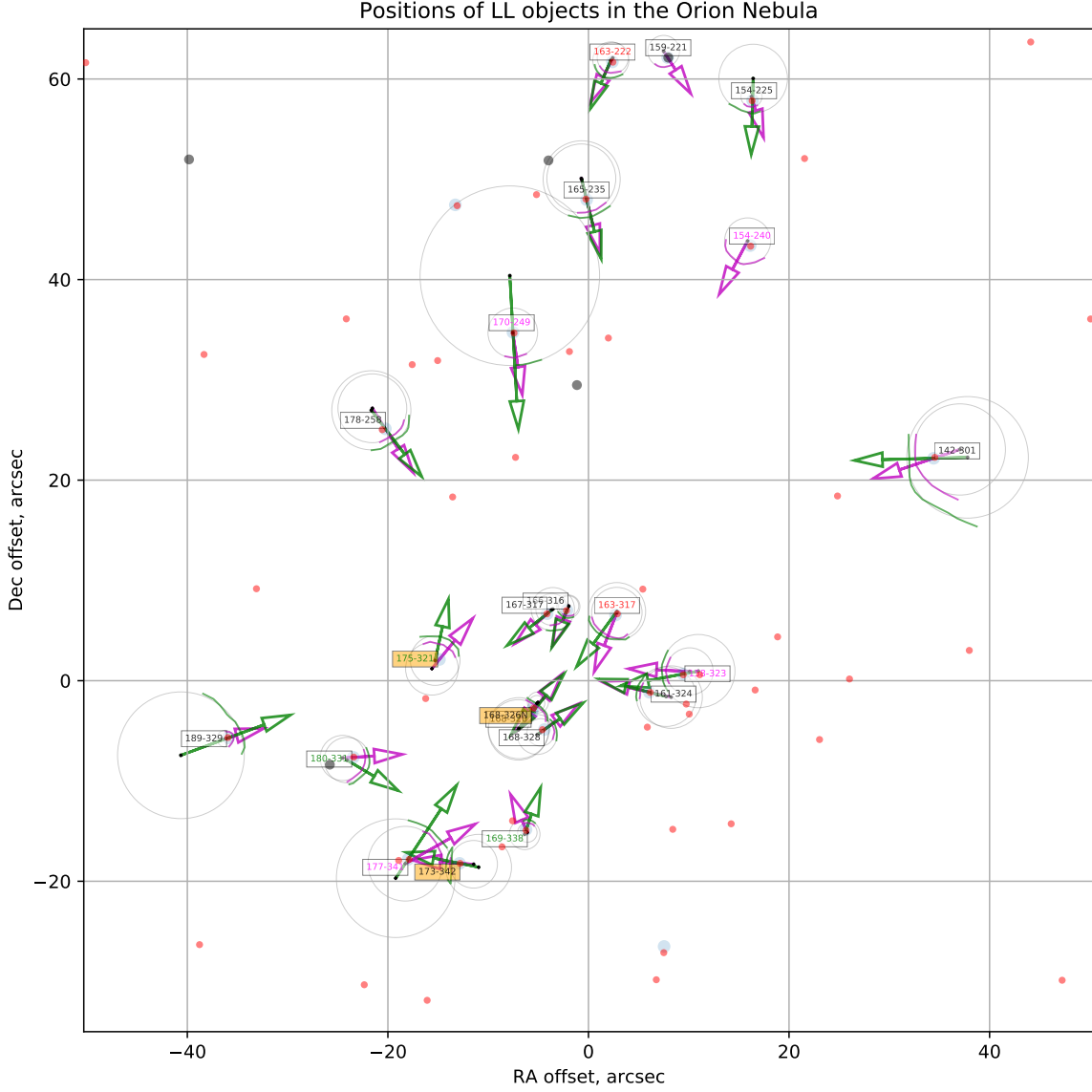


Figure 7. Position of bow shock arcs. Zoomed area.

154-225. The central source was previously catalogued as elongated body with diffuse boundary (O'Dell & Wong 1996). Later, Ricci et al. (2008) reported it as proplyd in a binary system (the main body). The central source is surrounded by a very faint and lumpy emission arc.

154-240. The central source is a large bright proplyd (Bally et al. 2000; Ricci et al. (2008) with a 3'' long tail and the inclined protoplanetary disk is seen in silhouette (Bally et al. 2000). There is evidence of an emission arc associated with

this proplyd, but only the inner edge can be clearly traced. The outer edge of the shell merges with a thick knotty structure whose origin is unclear.

159-221. This central source was first classified as a star by O'Dell & Wong (1996). This same source was reported as a dark disk seen only in silhouette by Ricci et al. (2008). But a faint emission rim can be seen surrounding the disk in the H α image, suggesting that it is an externally ionized proplyd. We identified an emission arc associated with the central star. The

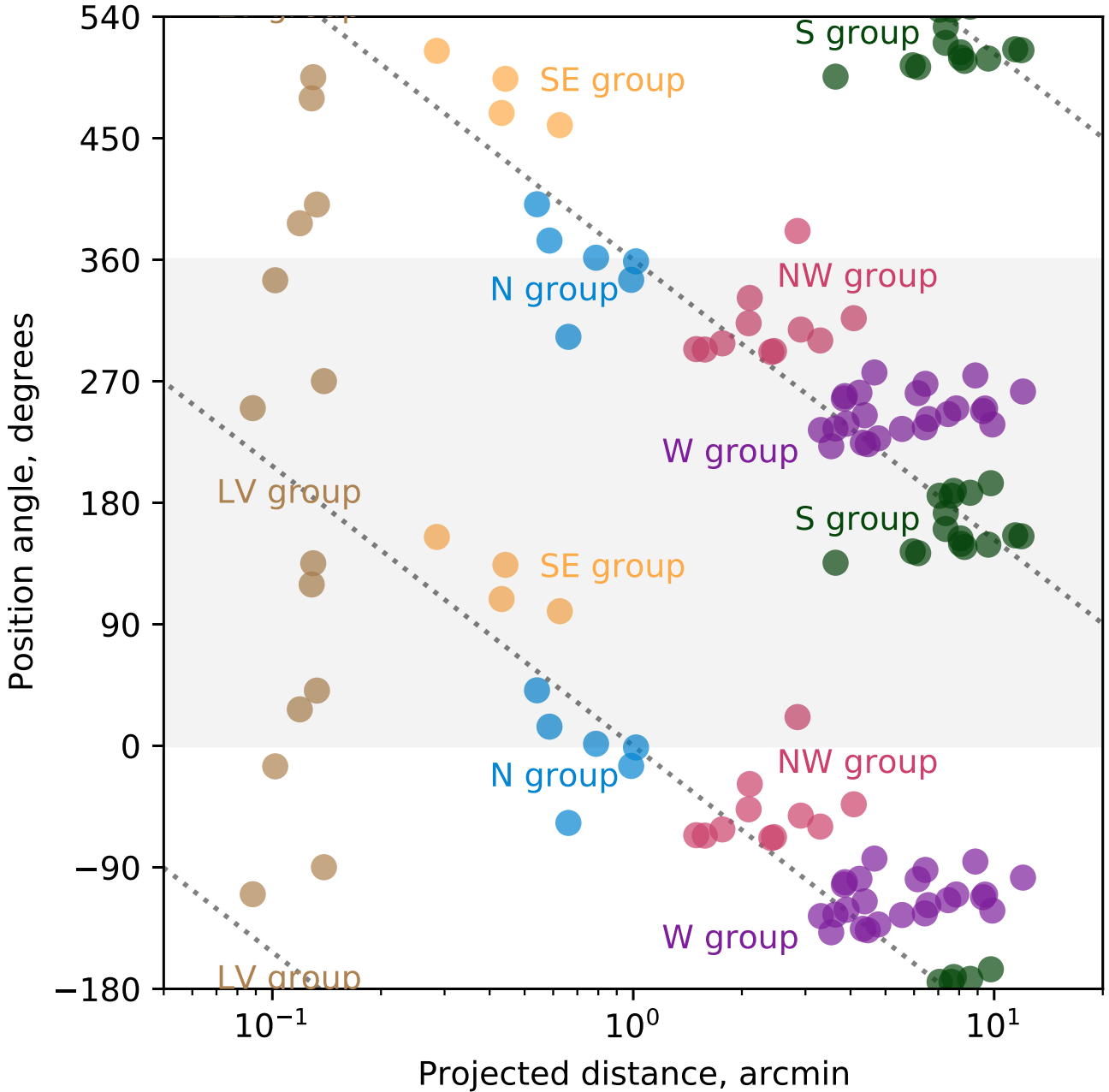


Figure 8. Position angle of bow shock location as a function of distance, both measured from θ^1 Ori C.

outer edge of the shell is very diffuse, which makes it difficult to trace of outer rim. The axis of the bowshock is significantly deviates from the radial direction.

163-222. The central proplyd was first catalogued by O'Dell & Wong (1996). There is a compact 0.''15 diameter disk seen nearly in face-on embedded in this stubby proplyd (Bally et al. 2000; Ricci et al. 2008). This source was also reported as a binary system (Ricci et al. 2008). An a very faint and small emission arc wraps the proplyd. The outer and

inner edges of the shell are well-defined on the eastern side, nevertheless the western side is superimposed on an unrelated a brighter larger scale emission filament, making impossible to trace the arc boundaries on this side.

165-235. This was previously catalogued as a star by O'Dell & Wong (1996). Later, It was classified as proplyd by Ricci et al. (2008). This proplyd is sorrounde by a previously uncatalogued emission arc. This emission arc is very faint.

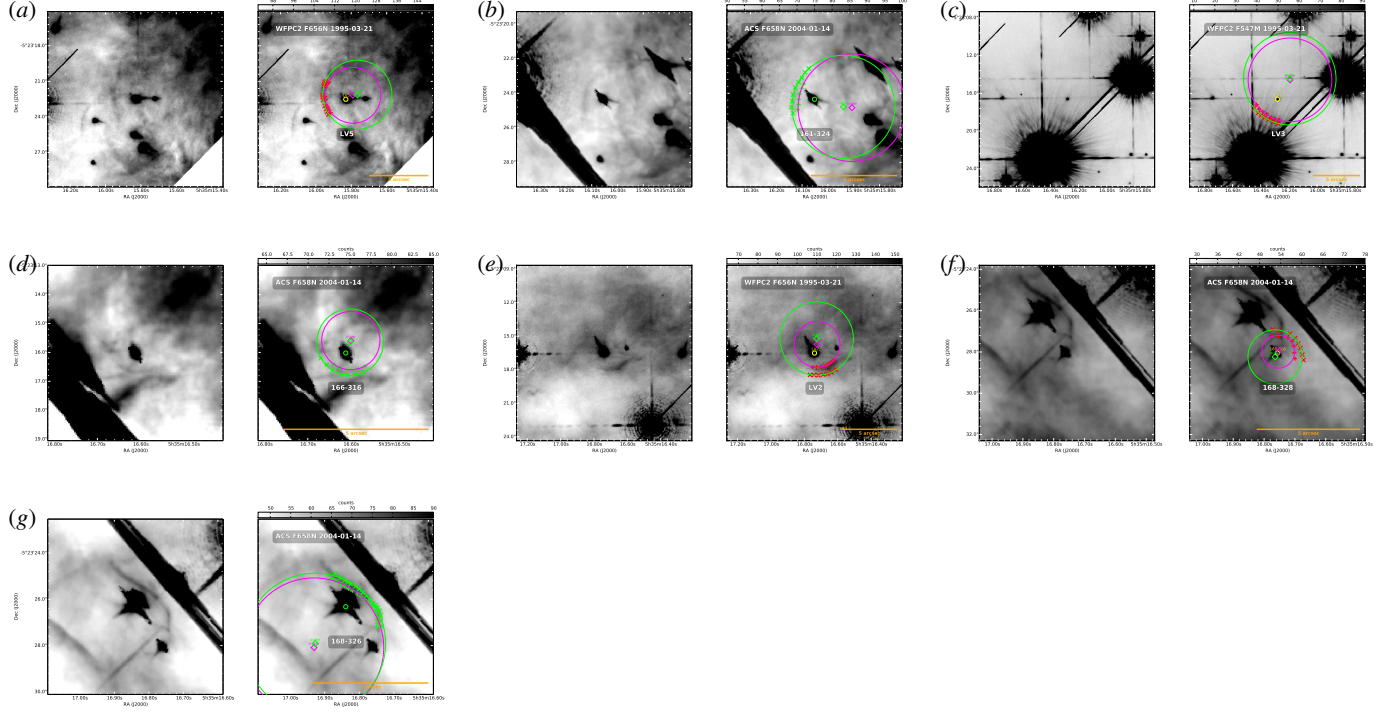


Figure 9. Stationary arc sources in the LV knots group.

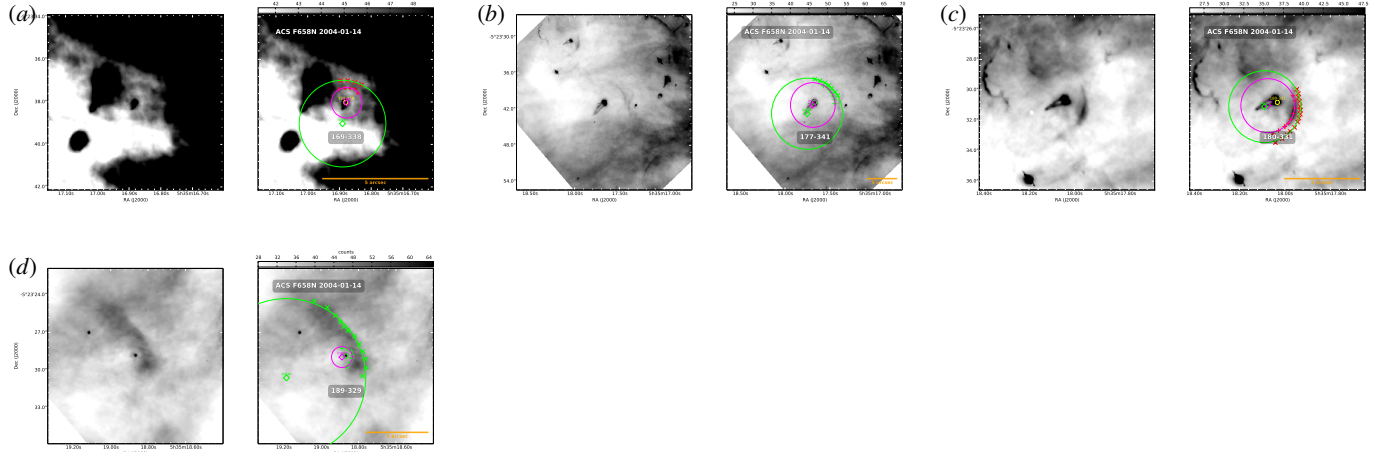


Figure 10. Stationary arc sources in the Southeast group.

170-249. This central source is a previously catalogued proplyd (O'Dell & Wong 1996), reported as a binary system by Ricci et al. (2008). This bright and large proplyd exhibits a long tail and an inclined disk seen in silhouette (Bally et al. 2000). Several filamentary emission features with arc shape crosses the object, nonetheless it is possible to identify a very faint emission arc that seems to be associated to the proplyd.

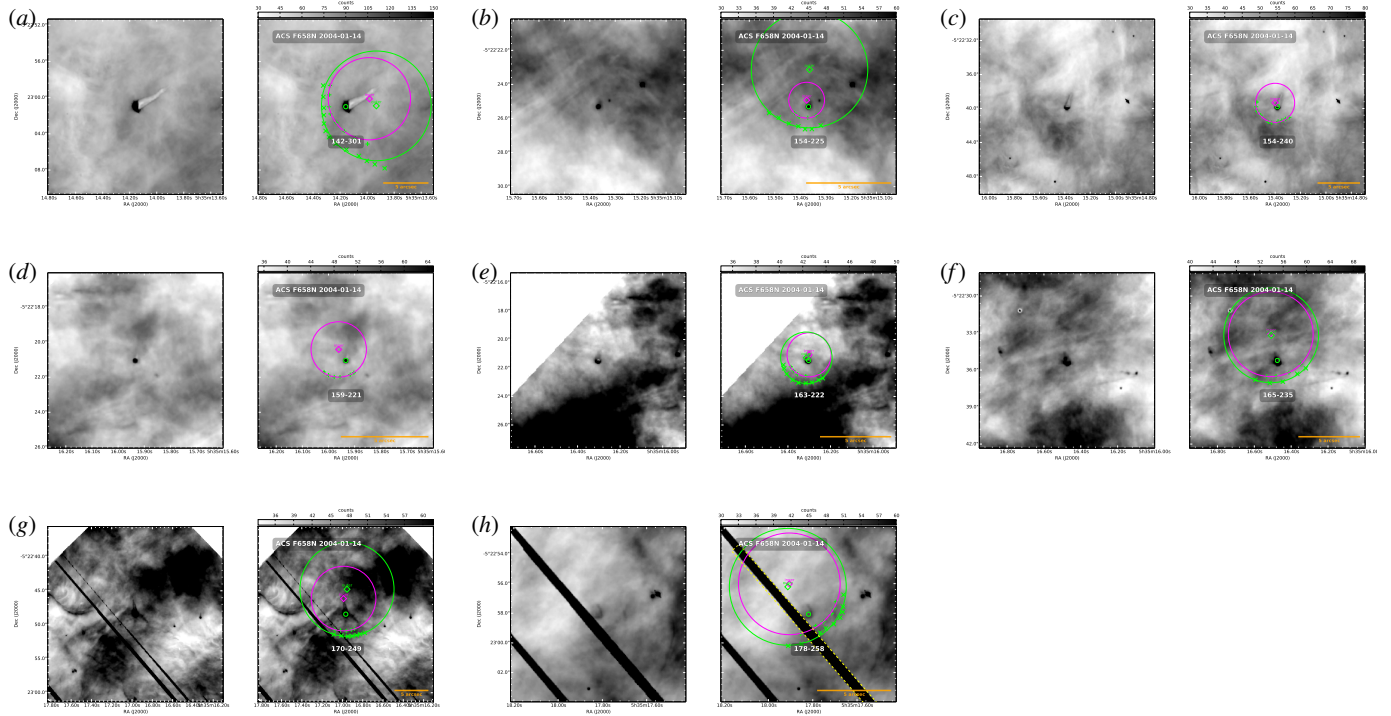
178-258. This large and weak proplyd was catalogued by Ricci et al. (2008), which is surrounded by a well-defined but faint emission arc.

3.4. Northwest group

The bowshock northwest group is located to the outskirt of the Orion Nebula. The mostly the emission arcs this group have been reported in the literature, with the exception of the 073-227 arc, which it was already previously reported.

Table 4. Shell geometric parameters of north group

| Object | RA | Dec | <i>D</i> | PA | R_{out} | R_{in} | Π_{out} | Π_{in} | Δ_{out} | Δ_{in} | h | PA_{out} | PA_{in} | Star ID | |
|---------|-------------|-------------|----------|-------|------------------|-----------------|--------------------|-------------------|-----------------------|----------------------|------|--------------------------|-------------------------|----------|----------|
| 142-301 | 05:35:14.16 | -05:23:01.0 | 39.67 | 122.9 | 2.42 | 1.82 | 4.33 | 16.20 | 1.90 | 4.78 | 0.60 | 91.5 | 98.6 | ACS 3847 | |
| 154-225 | 05:35:15.37 | -05:22:25.3 | 59.22 | 165.1 | 1.29 | 0.64 | 1.44 | 1.98 | 1.84 | | 0.58 | 158.0 | 193.1 | ACS 4106 | |
| 154-240 | 05:35:15.38 | -05:22:39.8 | 45.30 | 160.6 | | 1.72 | | 2.09 | | 1.38 | | | 202.3 | ACS 4112 | |
| 159-221 | 05:35:15.93 | -05:22:21.0 | 61.86 | 173.7 | | 0.83 | | 1.56 | | 1.46 | | | 215.4 | ACS 4285 | |
| 163-222 | 05:35:16.30 | -05:22:21.5 | 61.07 | 178.8 | 1.54 | 1.11 | 1.37 | 1.63 | 1.16 | | 0.36 | 198.9 | 180.1 | ACS 4398 | |
| 165-235 | 05:35:16.48 | -05:22:35.2 | 47.33 | 181.5 | 1.78 | 1.23 | 2.17 | 2.50 | | | 0.47 | 197.5 | 193.2 | ACS 4487 | |
| 170-249 | 05:35:16.97 | -05:22:48.4 | 35.16 | 194.2 | 3.23 | 2.45 | 1.61 | 1.28 | | | 0.78 | 173.4 | 193.3 | ACS 4586 | |
| 178-258 | 05:35:17.82 | -05:22:58.1 | 32.47 | 221.1 | 1.48 | 0.92 | 2.75 | 4.56 | | | 2.19 | 0.52 | 218.7 | 210.3 | ACS 4845 |

**Figure 11.** Stationary arc sources in the North group.

4578-251. This is a very bright T Tauri star associated with an emission arc that presents a double-shell morphology. This object has an asymmetric bow shock and the shell is more extended toward the south than to the north. The emission of the outer shell is fainter than the inner shell and is unclear whether the region marked with points is part of the outer shell.

049-143. Figure shows a proplyd (Ricci et al. 2008) with a very diffuse arc of emission. Its shell is thick, the wings of the bow shock are very open, and circular shaped. The inner edge is more diffuse than the outer edge and the bow shock is

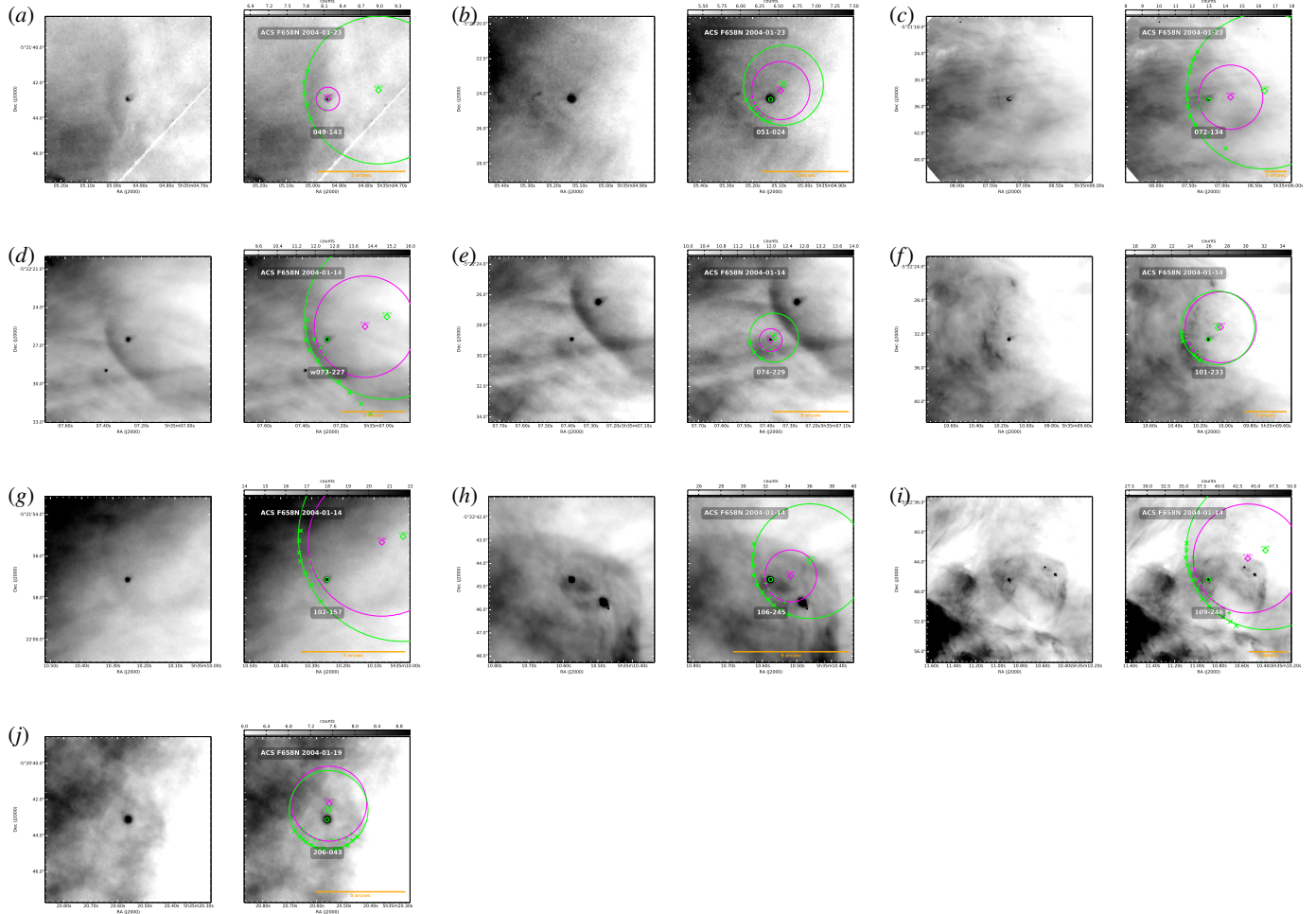
asymmetric. The proplyd has a short tail, probably indicating that it is highly inclined and there is extinction in the center.

051-024. We identified a previously uncataloged proplyd with its bow shock located in front of the upper end of the North Bright Bar. The emission shell is thin, but a second larger, and more diffuse, emission shell is seen in front of the bow shock that we have marked. It is unclear whether this outer shell is related to the object or not. If it is, then the object would be similar to the nearby 072-134.

072-134. This object is located to the southeast from 051-134. It was first cataloged by O'Dell & Wong (1996) and designated as 072-135. Later, Ricci et al. (2008) listed it as

Table 5. Shell geometric parameters of northwest group

| Object | RA | Dec | <i>D</i> | PA | R_{out} | R_{in} | Π_{out} | Π_{in} | Λ_{out} | Λ_{in} | h | PA_{out} | PA_{in} | Star ID |
|----------|-------------|-------------|----------|-------|------------------|-----------------|--------------------|-------------------|------------------------|-----------------------|-------|--------------------------|-------------------------|----------|
| 049-143 | 05:35:04.94 | -05:21:42.9 | 197.82 | 120.2 | 1.17 | 0.62 | 2.63 | 1.06 | 1.10 | 0.56 | 103.1 | 139.0 | ACS 2608 | |
| 051-024 | 05:35:05.13 | -05:20:24.3 | 245.01 | 136.7 | 1.19 | 0.90 | 1.83 | 1.65 | 1.77 | 2.14 | 0.27 | 136.5 | 123.6 | ACS 2628 |
| 072-134 | 05:35:07.20 | -05:21:34.3 | 174.74 | 128.3 | 4.69 | 2.26 | 2.81 | 2.80 | 2.10 | 2.50 | 2.42 | 89.7 | 94.5 | ACS 2840 |
| w073-227 | 05:35:07.27 | -05:22:26.5 | 147.27 | 112.4 | 1.63 | 0.81 | 2.41 | 3.41 | 2.86 | 3.31 | 0.70 | 117.0 | 120.5 | ACS 2842 |
| 074-229 | 05:35:07.38 | -05:22:28.9 | 144.78 | 111.7 | 1.36 | 0.79 | 1.15 | | | | 0.60 | 120.3 | 185.7 | ACS 2854 |
| 101-233 | 05:35:10.13 | -05:22:32.6 | 105.94 | 118.1 | 2.46 | 2.11 | 2.25 | 1.95 | | | 0.42 | 131.4 | 136.6 | ACS 3172 |
| 102-157 | 05:35:10.25 | -05:21:57.1 | 125.30 | 133.0 | 0.80 | 0.40 | 8.14 | 4.22 | 3.17 | 2.56 | 0.45 | 118.5 | 116.6 | ACS 3192 |
| 106-245 | 05:35:10.58 | -05:22:44.7 | 94.70 | 113.5 | 0.63 | 0.23 | 2.99 | 3.27 | 2.54 | 2.69 | 0.38 | 122.7 | 99.0 | ACS 3241 |
| 109-246 | 05:35:10.90 | -05:22:46.3 | 89.68 | 113.8 | 1.95 | 1.32 | 6.73 | 10.33 | 3.08 | 3.11 | 0.70 | 112.9 | 119.5 | ACS 3294 |
| 206-043 | 05:35:20.56 | -05:20:43.1 | 171.16 | 201.3 | 1.61 | 1.12 | 1.33 | 1.91 | | | 0.44 | 176.1 | 182.7 | ACS 5514 |

**Figure 12.** Stationary arc sources in the Northwest group.

disk seen nearly edge-on, named 072-135. In this work a shell with a complex morphology is identified. The inner edge is a narrow bright arc, while the shell is thick and faint, which is only visible on the N side.

073-227. [Bally et al. \(2000\)](#) reported a wind collision front associated with 073-227. The well-defined outer edge of the arc deviates significantly from the circular fit in the south wing of the bowshock.

074-229. This central source is located at south east of 073-227. It is a T Tauri star, that appears to be the smaller twin of the nearby 073-227, associated with a small and faint emission bow shock. The central star is not obviously a proplyd, but this may be because it is too small to be resolved. The projected separation from 072-134 is about 8''.0, which is not significantly smaller than the expected mean projected separation between nearest neighbors given the stellar density at this distance from the Trapezium ([Reipurth et al. 2007](#)), so the evidence that they form a physical binary pair is weak.

101-233. The central source was first cataloged as proplyd by [O'Dell & Wong \(1996\)](#), designated as 102-233, and later by [Ricci et al. \(2008\)](#) with the same name. This proplyd is associated with a clumpy, thin and low ionization bow shock. Several additional broad filamentary emission features can be seen in front of the arc, but it is unclear if these are associated with the object or are a chance superposition, that also seem to be aimed toward Trapezium.

102-157. We identified a previously uncataloged proplyd associated with a very faint emission arc. The proplyd tail is very short, indicating that it is highly inclined. 102-157 has a open bow. The southwest wing of the bowshock is crossed by an apparently unrelated east-west oriented filament, which makes it difficult to trace the emission arc on this side.

106-245 and 109-246. The bright proplyd 109-246 ([Ricci et al. 2008](#)) was previously cataloged as 109-247 by [Bally et al. \(2000\)](#), who noted its central dark disk and possible microjet. The proplyd is situated just outside the HH 202 bow shock and is superimposed on a complex background of fainter HH bow shocks that point towards the north west. However, a south-east facing bow shock is also clearly visible just in front of the proplyd. We identify this as a stationary arc due to its symmetric placement with respect to the proplyd axis and clear morphological differences from the HH bow shocks.

A similar, albeit much smaller arc can be seen in front of the stellar source 106-245. Given the complex nebular background, the evidence for an arc is not overwhelming, but is strengthened by the morphological similarity with the nearby 109-246. As with 074-249, the source is not obviously a proplyd, but again this may be simply due to its small size.

132-053. Similar area to 131-046, and also may be affected by extinction filaments. The shell looks more convincing in this object however, particularly the innner edge.

206-043. This object appears to show an extremely faint emission arc. However, it is seen against a strongly variable nebula background and a filamentary foreground extinction feature is seen nearby ($\approx 3''$ to west). It is therefore possible that the apparent arc is merely an illusion caused by an extension of these extinction filaments. Although it is not cataloged as a proplyd, the central source shows indications of a faint conical tail, pointing almost due North, with a length $\approx 2''$.

3.5. West group

This sparsely populated group is located in the outskirts of the Orion Nebula. The mostly of its members are the tipycal LL Ory arcs, with its well-defined emission arc.

4582-635. This is a previously cataloged proplyd ([Ricci et al. 2008](#)), which is surrounded by a very faint emission arc that has not been reported previously in the literature. There are hints of additional emission knots in front of the arc, but the S/N is very low and it is unclear if they are related with the object.

4596-400. [Bally et al. \(2000\)](#) first reported this object as a “wind collision front” with the designation 000-400. The central source was identified as a proplyd by [Ricci et al. \(2008\)](#), who gave it the designation 4596-400 based on more accurate astrometry, which we adopt here. The outer edge of the wings of the emission arc can be traced to much farther distances than is typical, at least 5 times the axial radius of curvature. The northern wing appears knotty at large distances, whereas the southern wing is smooth. However, the knots seen superimposed on the northern wing may be due to an unrelated, larger scale filament that crosses both this object and 012-407, which is most prominent in blue/green continuum filters.

000-400. [Bally et al. \(2000\)](#) reported a wind collision fronts associated with w000-400. The central source is a previously catalogued proplyd, designated 4596-400 ([Ricci et al. 2008](#)). The outer edge of the wings of the emission arc can be traced to much farther distances than is typical, at least 5 times the axial radius of curvature. The northern wing becomes knotty at large distances, where the southern wing is smoothes. The bow shock has parabolic morphology and wraps around a proplyd (Fig.).

005-514. This proplyd was first cataloged by [O'Dell & Wong \(1996\)](#). Later, [Bally et al. \(2000\)](#) reported a fainter and smaller wind-wind collision front, designated w005-514 and was show in $H\alpha$ image. The lower (southeast) wing of the arc has a complex structure, with multiple overlapping filaments.

012-407. [Bally et al. \(2000\)](#) reported a wind collision fronts associated with 012-407. The bright central star is not obviously a proplyd. The diffuse shell is very thick.

014-414. [Bally et al. \(2000\)](#) cataloged another wind collision front associated with 014-407. It is one of the smaller LL arcs in this group, containing a double central star. A larger

Table 6. Shell geometric parameters of west group

| Object | RA | Dec | D | PA | R_{out} | R_{in} | Π_{out} | Π_{in} | Λ_{out} | Λ_{in} | h | PA_{out} | PA_{in} | Star ID |
|----------|-------------|-------------|--------|------|------------------|-----------------|--------------------|-------------------|------------------------|-----------------------|------|--------------------------|-------------------------|----------|
| 4285-458 | 05:34:28.52 | -05:24:57.9 | 721.18 | 82.4 | 1.91 | | | | | | | | 87.0 | ACS 372 |
| LL3 | 05:34:40.81 | -05:26:38.5 | 566.33 | 69.8 | 3.12 | 1.28 | 1.90 | 2.59 | 1.79 | 2.68 | 1.83 | 89.2 | 99.6 | ACS 967 |
| LL2 | 05:34:40.86 | -05:22:42.2 | 532.12 | 94.3 | 4.04 | 2.07 | 4.20 | 5.02 | 3.89 | 3.30 | 1.13 | 97.6 | 89.5 | ACS 973 |
| 4417-653 | 05:34:41.70 | -05:26:52.9 | 559.12 | 67.9 | 1.19 | 0.72 | 3.94 | 4.31 | 3.19 | 3.20 | 0.45 | 57.3 | 49.8 | ACS 1025 |
| LL4 | 05:34:42.72 | -05:28:37.2 | 593.11 | 58.0 | 2.42 | 1.42 | 3.08 | 3.31 | 2.90 | 2.97 | 0.99 | 46.7 | 40.3 | ACS 1086 |
| 4468-605 | 05:34:46.76 | -05:26:04.8 | 471.30 | 69.9 | 2.47 | 1.33 | 2.20 | 1.81 | 2.03 | 1.46 | 1.20 | 54.2 | 59.6 | ACS 1351 |
| 4491-627 | 05:34:49.07 | -05:26:26.5 | 447.58 | 65.7 | 2.02 | 1.19 | 2.43 | 2.03 | 1.99 | 1.42 | 0.79 | 72.3 | 76.4 | ACS 1566 |
| 4505-336 | 05:34:50.49 | -05:23:35.3 | 386.95 | 88.1 | 1.62 | 0.93 | 2.02 | 3.21 | 1.92 | 2.34 | 0.66 | 99.8 | 99.5 | ACS 1654 |
| 4520-419 | 05:34:52.01 | -05:24:18.7 | 368.41 | 81.2 | 1.39 | 1.07 | 2.60 | 2.83 | | | 0.32 | 84.3 | 85.2 | ACS 1754 |
| 4531-628 | 05:34:53.07 | -05:26:27.6 | 394.31 | 62.0 | 0.79 | 0.46 | 1.30 | 2.05 | | | 0.33 | 104.0 | 89.0 | ACS 1831 |
| 4550-659 | 05:34:55.01 | -05:26:58.8 | 385.57 | 55.9 | 1.61 | 0.88 | 3.48 | 8.09 | 3.10 | 4.06 | 0.45 | 68.1 | 71.8 | ACS 1938 |
| 4578-251 | 05:34:57.79 | -05:22:51.1 | 279.49 | 96.5 | 1.85 | 1.19 | 1.91 | 1.33 | 1.63 | 1.38 | 0.53 | 81.2 | 125.0 | ACS 2106 |
| 4582-635 | 05:34:58.17 | -05:26:35.1 | 333.37 | 54.7 | 1.11 | 0.68 | 3.27 | 2.64 | 2.15 | | 0.46 | 65.7 | 50.5 | ACS 2134 |
| w000-400 | 05:34:59.57 | -05:24:00.1 | 254.03 | 81.5 | 1.47 | 0.80 | 2.49 | 3.52 | 2.40 | 2.42 | 0.68 | 71.9 | 73.4 | ACS 2204 |
| w005-514 | 05:35:00.47 | -05:25:14.3 | 262.72 | 64.8 | 1.65 | 1.20 | 1.52 | 1.76 | 1.73 | 1.60 | 0.44 | 64.5 | 57.9 | ACS 2244 |
| w012-407 | 05:35:01.17 | -05:24:06.7 | 231.47 | 79.0 | 2.29 | 0.95 | 2.59 | 2.52 | 2.07 | 2.31 | 1.23 | 68.3 | 69.7 | ACS 2313 |
| w014-414 | 05:35:01.37 | -05:24:13.4 | 229.95 | 77.2 | 1.21 | 0.37 | 1.62 | 77.64 | 1.61 | 3.05 | 0.70 | 98.3 | 93.2 | ACS 2309 |
| 022-635 | 05:35:02.20 | -05:26:35.3 | 286.47 | 47.7 | 1.10 | 0.75 | 3.65 | 3.10 | | | 0.34 | 83.2 | 77.5 | ACS 2385 |
| w030-524 | 05:35:03.00 | -05:25:24.4 | 234.09 | 58.6 | 0.63 | 0.29 | 4.28 | 109.64 | 2.83 | | 0.32 | 93.8 | 82.0 | ACS 2439 |
| 041-637 | 05:35:04.06 | -05:26:37.1 | 267.84 | 43.4 | 1.94 | 1.19 | 2.10 | 4.45 | 1.79 | 2.38 | 0.77 | 4.2 | 15.5 | ACS 2507 |
| 042-628 | 05:35:04.20 | -05:26:27.6 | 259.59 | 44.5 | 3.07 | 1.76 | 1.81 | 1.95 | 1.90 | 1.81 | 1.34 | 61.6 | 56.1 | ACS 2526 |
| w044-527 | 05:35:04.43 | -05:25:27.4 | 217.94 | 55.0 | 2.13 | 0.78 | 3.02 | 11.90 | | | 0.85 | 121.2 | 267.4 | ACS 2543 |
| LL1 | 05:35:05.64 | -05:25:19.4 | 198.63 | 53.9 | 3.06 | 1.90 | 2.59 | 2.68 | 2.25 | 2.44 | 1.13 | 84.4 | 78.1 | ACS 2682 |
| w069-601 | 05:35:06.91 | -05:26:00.6 | 212.19 | 41.9 | 0.85 | 0.41 | 2.44 | 4.02 | 2.19 | 2.72 | 0.42 | 86.1 | 87.1 | ACS 2815 |

Table 7. Notes on Southwest Group

| Source | Proplyd | Star | Arc | Notes |
|----------|---------|------|-------|---|
| 4582-635 | R08 | ... | New | Very faint |
| 000-400 | R08 | ... | BOM00 | Designated 4596-400 in R08 |
| 005-514 | OW96 | ... | BOM00 | |
| 012-407 | No | ... | BOM00 | Thick, diffuse arc |
| 014-414 | No | ... | BOM00 | Double central star |
| 022-635 | No | ... | New | Asymmetric arc |
| 030-524 | ? | ... | BOM00 | Flat, asymmetric arc, apparent proplyd tail |

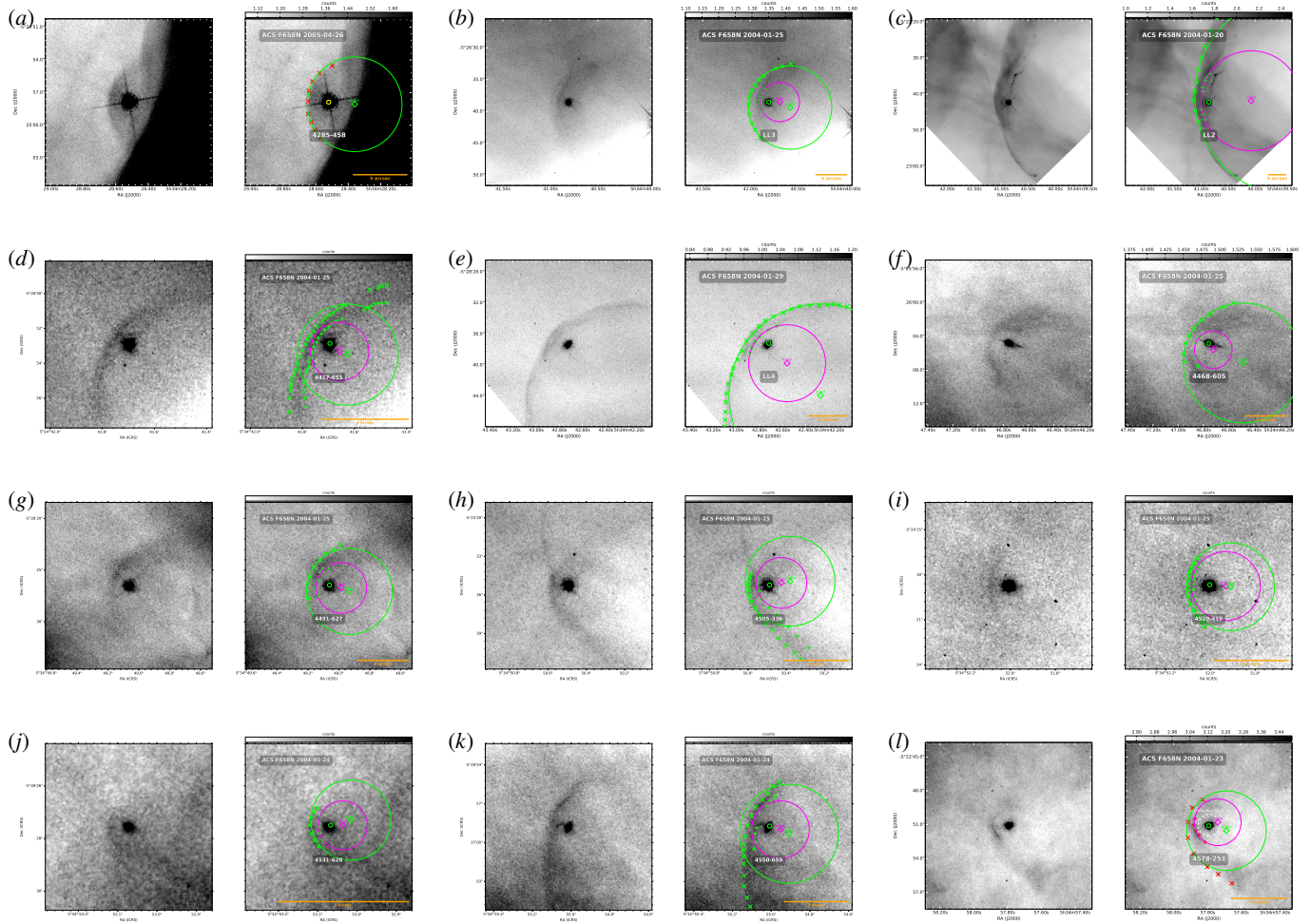


Figure 13. Stationary arc sources in the West group.

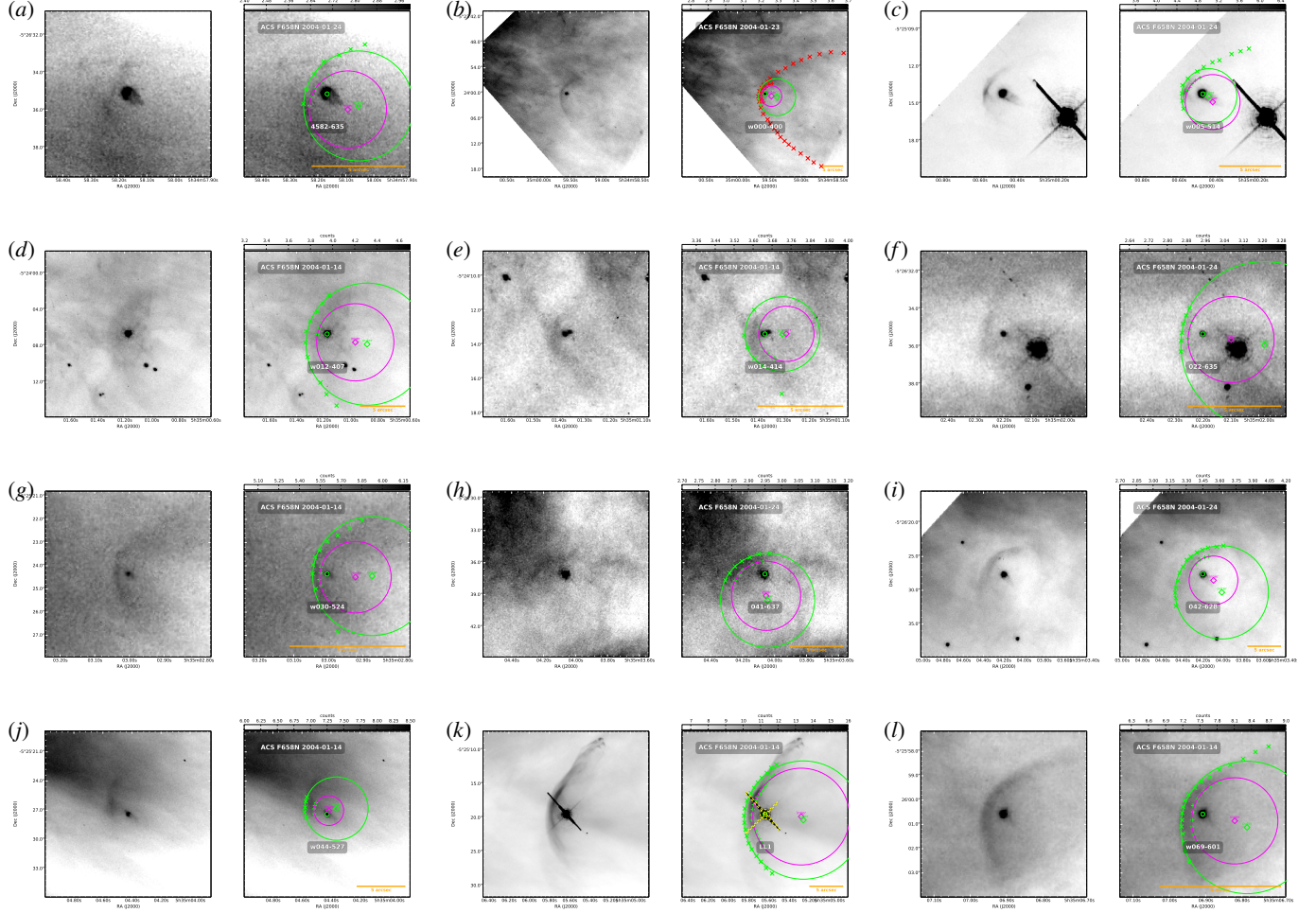


Figure 14. Stationary arc sources in the West group – continued.

scale filament which is prominent in blue/green continuum crosses the object, but seems to be unrelated.

022-635. This is a previously uncatalogued arc of emission that wraps around a T Tauri star. The north wing of the bowshock is more extended than south wing. There are two apparently unrelated emission filaments that cross this object.

030-524. Bally et al. (2000) reported a wind-wind collision front, associated with w030-524. The central source has a tail oriented away from the Trapezium, indicating a proplyd. The northern outer edge of the asymmetric shell is very flat and it makes a sharp corner where it joins the head of the shell.

041-637. This is a previously reported star (Da Rio et al. 2009) associated with a faint emission arc. There is a west faint emission arc, which is probably unrelated to the object. The emission arc has not been previously reported in the literature.

042-628. This source appears in the proplyd catalog of Ricci et al. (2008) with the designation 038-627, supposedly based on appearance in previous catalogs (O'Dell & Wong 1996). However, we have been unable to locate the source in

any other catalogs and the source coordinates clearly indicate a designation of 042-628, which we adopt here. A bright compact knot is seen just inside the emission arc, $\approx 2''$ to the north of the proplyd, which may represent a jet. A fainter knot is also seen closer to the proplyd, but at a slightly larger position angle.

044-527. A faint and small emission arc associated with 044-527 was cataloged by Bally et al. (2000). The central source was subsequently classified as proplyd by Ricci et al. (2008). This object has a jet parallel to the proplyd axis. The bowshock is very asymmetric.

LL 1 (056-519). The T Tauri star LL Orionis is the prototype of the LL objects. Its emission arc was discovered by Gull & Sofia (1979) and is now denoted LL 1. This is a parabolic or hyperbolic bowshock that wraps around the source star (Bally et al. 2006). This emission arc was also reported by Bally et al. (2000) and as a LL Orionis-type wind-wind collision front LL 1 by Bally & Reipurth (2001). The emission of the bowshock wings is blueshifted with respect to the background nebular emission, the emission from the head of the bowshock

is at a similar velocity to the nebula and shows no detectable proper motion, consistent with it being a stationary structure (Henney et al. 2013). LL 1 is associated with a hypersonic jet Herbig-Haro, HH 888, that arises in the T Tauri star.

069-601. This was first classified as a non-proplyd stellar source by O'Dell & Wong (1996). Later, a wind collision front was reported by Bally et al. (2000) associated with w069-601. Ricci et al. (2008) catalogued the central source as a proplyd. The parabolic arc emission is well-defined, which makes it easy to trace the edges of the shell. The arc shape is very similar to LL 1, but is considerably smaller.

4285-458. This is an emission arc that wraps a bright T Tauri star. Although the outer boundary of the shell is well-defined, it is impossible to trace the shell's inner boundary due to confusion with the PSF wings of the central star. This is the most distant emission arc from the Trapezium in this catalog and It is also much smaller than the other arcs in the west group.

LL 3 (4408-639). This previously reported LL Ori-type object (Bally & Reipurth 2001) exhibits a double-shell morphology to the emission arc: an inner shell that is brighter and narrower, and an outer shell that is fainter and broader, but still with a well-defined outer edge. In addition, the central star shows a faint emission structure, which protrudes to the WSW, and which may represent a proplyd tail, although the object is not included in any proplyd catalogs, such as Ricci et al. (2008).

LL 2 (4409-242). This large LL Ori-type object (Bally & Reipurth 2001), is associated with the T Tauri star IX Ori. It also has a bipolar jet, HH 505, which is oriented nearly perpendicular to the bowshock axis. Apart from LL 1, this is the only LL object whose kinematics have been studied via spectroscopic mapping (Henney et al. 2013). Unlike LL 1, the structure and kinematics of the LL 2 arc are very asymmetrical. Additionally, proper motion studies (Henney et al. 2013) show that only the head and northern wing of the arc are stationary structures: the southern portion of the arc has high proper motion and seems to be driven by the blueshifted jet.

4417-653. This is a star previously catalogued by Hillenbrand (1997). There is an emission arc associated with this source. The shock has not been reported in the literature. This object is located 20 arcsec to the southeast of LL 3 and their arcs have very open wings.

LL 4 (4427-838). This is a previously reported LL Ori-type object (Bally & Reipurth 2001). The central source was reported as a proplyd and a binary system by Bally et al. (2006). At first glance, this object appears to be a single arc with a very large radius of curvature. However wide closer inspection suggests that the "wings" of the arc are separate structures from the more curved nose region. We suggest that they may not be part of the true LL arc, but are instead driven

by the bipolar jet (Bally et al. 2006) in a similar way to the southern wing of LL 2.

4468-605. This arc was first reported by Bally et al. (2006) who also noted the proplyd nature of the central source and the presence of a microjet (HH 886) oriented approximately parallel to the symmetry axis of the proplyd and arc. Although Bally et al. (2006) report the jet as one-sided, a bright H α filament seen at the end of the proplyd tail may represent the counterjet. The north side of the emission arc shows an apparent flared morphology, but this may be illusory, due to an unrelated larger scale emission filament that is projected against that side of the bowshock.

4491-627. This is a pre-main-sequence star catalogued by Parihar et al. (2009). The shock associated with this source has not been listed previously. It is a small and faint arc.

4505-336. The star associated with the shock was catalogued by Hillenbrand (1997). The arc has not been reported in the literature. The north wing of the arc is not visible. A very faint jet seems to go north of the star. It probably ends in a bow shock.

4520-419. The stellar component was previously reported by Parihar et al. (2009). This pre-main-sequence star might be a proplyd because it appears to have a small tail. The associated arc has not been reported in the literature. It is a very weak arc with a circular and symmetric shape.

4531-628. This object is a pre-main-sequence star (Da Rio et al. 2009) which has associated an emission arc that has not been previously reported. It is a very small and faint arc.

4550-659. This source was previously catalogued as a pre-main-sequence star by Parihar et al. (2009). The arc associated with this star has not been reported in the literature. It is a large arc with very open wings. It seems that two jets arise in the stellar component. A bright jet to the northwest and a smaller one to the southeast of the star.

3.6. South group

The bowshock south group is located in the outskirts of the Orion Nebula and southeast of the Bright Bar, several members of this group are the farthest objects from the Trapezium. The objects are generally large in this group and many have a bright inner rim.

066-3251. This object was classified as a proplyd by Ricci et al. (2008) and, located at a distance $\sim 10'$ south of the ONC core, it is one of the farthest known proplyds from the Trapezium. We have identified a faint arc associated with this proplyd, which is seen most clearly in the F555W broad band filter but is also visible in the H α filter. This object is projected onto the tip of a large-scale wishing bone shaped filament, which seems to represent a local ionization front. We believe that the "outflow", which Ricci et al. (2008) identify to the south of this object is merely a misidentification of part of this filament.

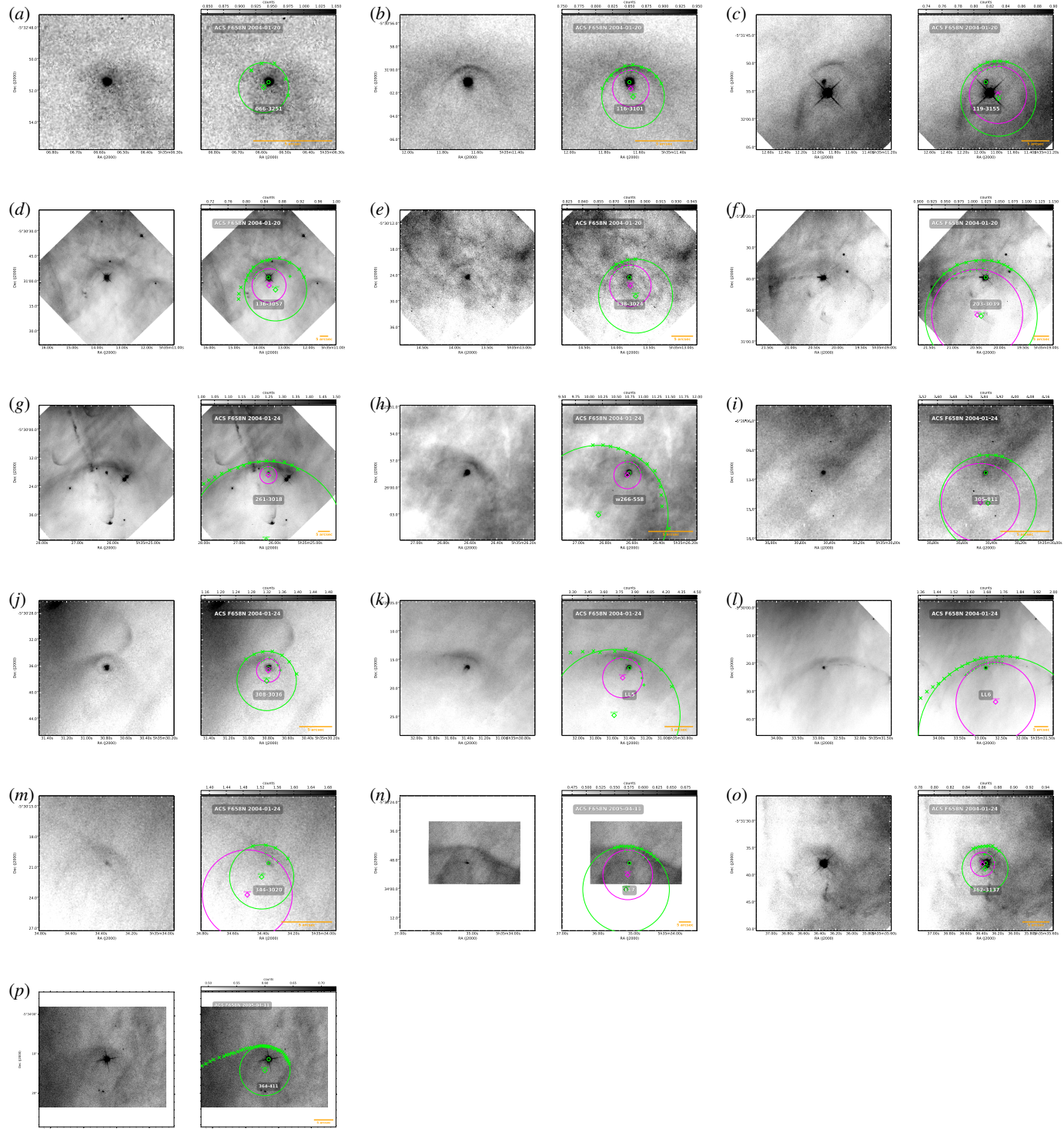


Figure 15. Stationary arc sources in the South group.

Table 8. Shell geometric parameters of south group

| Object | RA | Dec | <i>D</i> | PA | <i>R</i> _{out} | <i>R</i> _{in} | Π_{out} | Π_{in} | Λ_{out} | Λ_{in} | <i>h</i> | PA_{out} | PA_{in} | Star ID |
|----------|-------------|-------------|----------|-------|-------------------------|------------------------|--------------------|-------------------|------------------------|-----------------------|----------|--------------------------|-------------------------|----------|
| 066-3251 | 05:35:06.57 | -05:32:51.4 | 587.49 | 14.5 | 1.07 | | 1.49 | | 1.19 | | | 300.1 | | ACS 2787 |
| 116-3101 | 05:35:11.65 | -05:31:01.0 | 463.92 | 8.8 | 1.45 | 1.00 | 1.57 | 1.88 | 1.55 | 1.69 | 0.44 | 24.0 | 7.9 | ACS 3390 |
| 119-3155 | 05:35:11.93 | -05:31:53.3 | 515.10 | 7.4 | 3.02 | 1.95 | 1.70 | 2.65 | 1.62 | 2.04 | 1.00 | 33.3 | 35.3 | ACS 3438 |
| 136-3057 | 05:35:13.61 | -05:30:57.6 | 456.93 | 5.2 | 10.13 | 4.91 | 1.80 | 5.98 | 1.78 | 2.39 | 4.51 | 10.9 | 4.4 | ACS 3764 |
| 138-3024 | 05:35:13.80 | -05:30:24.4 | 423.64 | 5.2 | 3.89 | 2.74 | 1.96 | 1.66 | | 1.62 | 1.11 | 22.2 | 17.4 | ACS 3756 |
| 203-3039 | 05:35:20.29 | -05:30:39.4 | 440.72 | 352.4 | 5.38 | 1.76 | 3.14 | 7.03 | 2.38 | 3.83 | 3.06 | 359.4 | 8.2 | ACS 5456 |
| 261-3018 | 05:35:26.17 | -05:30:18.0 | 440.40 | 340.6 | 4.99 | 2.51 | 7.35 | 1.55 | 4.02 | 3.33 | 2.59 | 1.7 | 357.1 | ACS 6473 |
| w266-558 | 05:35:26.62 | -05:25:58.3 | 218.16 | 315.6 | 1.88 | 1.13 | 5.42 | 1.32 | 2.16 | 2.07 | 0.78 | 330.7 | 298.5 | ACS 6559 |
| 305-811 | 05:35:30.44 | -05:28:11.2 | 356.86 | 324.0 | 1.72 | 0.89 | 3.63 | 6.57 | | | 0.80 | 358.6 | 349.7 | ACS 7023 |
| 308-3036 | 05:35:30.79 | -05:30:36.3 | 484.13 | 333.6 | 2.56 | 1.44 | 1.61 | 1.09 | 1.62 | 1.08 | 1.12 | 359.9 | 329.8 | ACS 7074 |
| LL5 | 05:35:31.40 | -05:28:16.4 | 369.54 | 322.7 | 2.96 | 1.46 | 2.26 | 2.23 | 2.81 | 1.98 | 1.49 | 339.7 | 339.7 | ACS 7161 |
| LL6 | 05:35:32.87 | -05:30:21.5 | 485.82 | 329.6 | 3.63 | 1.63 | 6.01 | 4.90 | 3.72 | 4.17 | 2.05 | 7.6 | 18.0 | ACS 7338 |
| 344-3020 | 05:35:34.36 | -05:30:20.6 | 496.76 | 327.3 | 1.66 | 0.67 | 2.17 | 4.82 | 2.23 | 2.45 | 0.95 | 334.9 | 325.5 | ACS 7458 |
| LL7 | 05:35:35.13 | -05:33:49.2 | 686.23 | 335.9 | 7.00 | 5.53 | | | | | 1.46 | 359.2 | 3.8 | ACS 7547 |
| 362-3137 | 05:35:36.35 | -05:31:37.8 | 577.96 | 329.0 | 3.12 | 1.57 | 1.32 | 1.41 | | 1.10 | 1.47 | 6.4 | 267.8 | ACS 7661 |
| 364-411 | 05:35:36.44 | -05:34:11.1 | 714.33 | 335.2 | 3.04 | | | | | | | 341.1 | | ACS 7676 |

116-3101. Figure shows a proplyd associated with a small but sharply defined emission arc. The central star is also named V488 Ori ([Bally et al. 2006](#)). The wings of the bow shock are very closed, the outer edge is well defined and has a circular shape since we can fit a perfect circle with the points marked.

119-3155. This is a binary system associated with an emission arc. Based on the position of the outer of curvature of the arc, we assign the fainter, more northern binary component as the corresponding stellar source. It has a faint arc to the north and another to the east (Fig), but the east arc is probably unrelated to the object, and may instead be associated with the HH 880 bowshock which passes 15'' to the south. This emission arc has not been previously reported in the literature.

136-3057. This is a T Tauri star associated with an emission arc. It is located to the north of 119-3155 and is one of the bigger objects of this group. 136-3057 has a very diffuse shell. This has not been previously reported in the literature.

138-3024. Figure shows a T Tauri star associated with a thin shell. The arc is seen most strongly blue and green broad band filters, but it is also seen at very low contrast in the H α filter. This object has not been previously reported in the literature.

203-3039. This object has a microjet (HH 561) which was discovered in the Fabry-Pérot study of the southern Orion Nebula by [Bally & Reipurth \(2001\)](#). Later, this HH object was described in more detail by [Bally et al. \(2006\)](#), the microjet emerges toward the east from the variable star MY Ori, terminating in a faint bowshock at a distance of 16''. A fainter counterjet and bowshock are located west of the star. In addition to these previously reported features, we identify an LL-type emission arc associated with MY Ori. The faint bow is very open.

261-3018. This is a relatively large and diffuse LL-type arc previously unreported, seen superimposed on a very complicated region of overlapping flows. We tentatively identify the star 261-3018 as the source, although the star (264-3016) is another possible candidate. In the H α the 261-3018 star (which is the same source as 262-3018 reported by [Bally et al. 2006](#)) shows a linear protrusion of length $\simeq 1''$ towards the southwest. This is unlikely to be a proplyd tail, since it is not aligned with the radial direction from the Trapezium, and instead may be a microjet. Indeed, a series of faint knots and bowshocks extend for 30'' in the same direction. The LL-type arc is very flat and shows a bright rim at its inner edge. It extends further to the east than to the west. The object is seen in projection superimposed on the HH 502 flow but shows no evidence of physical interaction with this flow.

266-558. [Bally et al. \(2000\)](#) catalogued a wind collision front associated with w266-558. Figure shows emission shell that wraps around the source. The source is a previously catalogued proplyd by [Ricci et al. \(2008\)](#). w266-558 presents

a double-shell morphology, with knotty bow wings. The bow wings are very open. Although, we have assigned this object to the south group, it is located much closer to the Trapezium than the other members, in a region lacking in other arcs.

305-811. Previously classified as LL-type object by [Bally et al. \(2006\)](#). The emission arc is extremely faint and asymmetric. The star shows a faint protrusion to the southeast in the H α filter, probably indicating a proplyd tail, although the source has not previously been catalogued as a proplyd.

308-3036. [Bally et al. \(2006\)](#) reported a bright star, that is surrounded by a faint arc of emission, located to the west of LL 6. This object has a nearly circular inner shock, the circle fit is roughly centered on the star. The circular silhouette (see Fig.) may trace a wind cavity, or possibly a dusty envelope surrounding the star ([Bally et al. 2006](#)).

LL 5 (315-816). This is a LL Ori type object identified in the outskirts of the Orion Nebula, it was first reported by [Bally & Reipurth \(2001\)](#). Later, it was also catalogued by [Bally et al. \(2006\)](#) and they mentioned that LL 5 is associated with the V1559 Ori star. This object has a short jet (HH 875 [Bally et al. 2006](#)) emerging from the proplyd toward the northeast. The emission arc wraps around a proplyd, and was designated LLP 315-816 or 314-816. This object has a double-shell morphology with a bright inner rim.

LL 6 (329-3021). ([Bally & Reipurth 2001](#)) identified a LL Orionis-type wind-wind collision fronts LL 6 in the outskirts of the Orion Nebula. LL 6 is associated with the star NX Ori, which is surrounded by a large arc of emission ([Bally et al. 2006](#)). The wings of the bowshock are very open and extended. This object has a prominent, one-sided jet, oriented perpendicular to the axis of the LL arc. It is difficult to distinguish between the wings of the LL arc and the jet-driven bowshocks.

344-3020. [Bally et al. \(2006\)](#) catalogued a proplyd associated with an emission arc, designated as LL 344-3020. This object is very faint and has a bipolar jet at P.A. = 45°.

LL 7 (351-3349). This object is a LL-type bowshock previously reported by [Bally & Reipurth \(2001\)](#). The central source is a previously catalogued proplyd ([Ricci et al. 2008](#)), designated 351-3349. This object has a jet at P.A. $\sim 80^\circ$ perpendicular to LL arc axis. The bowshock wings are very open, and it is one of the most distant emission arcs from the Trapezium in this catalog. This object is larger than we show, the bowshock from jet overlap wings of LL arc (see [Bally & Reipurth 2001](#)).

362-3137. This is a previously uncatalogued proplyd associated with an emission arc. However, [Da Rio et al. \(2009\)](#) catalogued the central source as a star. The source is a double star. It is located at north of LL 7. This object seems to show a double-shell morphology. There is a filament to south probably unrelated to the object. This emission arc has not been previously reported in the literature.

364-411. The star was catalogued by Hillenbrand (1997). The arc associated to this star has not been reported. The outer arc only can be traced, because the inner one can not be seen. It is located approximately 25 arcsec to the southeast of LL 7. Making of it the most distant arcs from the Trapezium.

3.7. Interproplyd shells

The interproplyd shell is a group of small proplyds, which they are associated with small emission arcs which are formed by the interactions between two individual photoevaporation flows.

160-350. This was previously reported as an irregular proplyd by O'Dell & Wen (1994) and was designated 159-350. Later, Ricci et al. (2008) cataloged it as a binary system and ionized disk seen in emission. The 159-350 outflow interact with the 160-350 flow producing a small emission arc.

162-456. O'Dell & Wong (1996) cataloged this object as a stellar source and designated it 162-457. It was listed as a pre-main-sequence binary star by Reipurth et al. (2007). A small emission arc is formed by the interaction of the flows come from 162-456 and 162-456NE, the latter located in the Northeast of 162-456.

168-326N. This source was previously reported as an unclear object due to saturation by O'Dell & Wen (1994). Later, it was catalogued as a proplyd and binary system by Ricci et al. (2008). Comparing the 5 GHz radio emission to the H α and [O III] λ 5007 emission is perceptive a radio source between southeast radio source 168-326SE and the northwest radio source 168-326NW. This structure is probably an interacting zone between the two components (Graham et al. 2002). From Fig. ?? in not possible to see any emission arc because the system is very affected by saturation.

173-342. This was classified as a semi-stellar and elongated object with diffuse boundary and appears designated 173-341 O'Dell & Wen (1994). This source was identified as a proplyd and binary system by Ricci et al. (2008). The emission arc is probably formed by the interaction of 173-342 with 177-341 (HST1). The arc emission shock in clearly visible in the image.

175-321. This was catalogued as a stellar source by O'Dell & Wong (1996). The emission arc is not produced by the interaction of two proplyd flows. However, the shock seems to be oriented towards th1D, which is very close to it. This arc has not been reported in the literature.

204-330. This source was previously reported as a proplyd and binary system by Ricci et al. (2008) on which appears with the designation 204-330. Due to the interaction between the flows of 204-330 and 205-330 proplyds is formed small and faint emission arc. This shock has also not been reported in the literature.

3.8. Ambiguous objects

065-502. This was classified as a non-propolyd stellar source by O'Dell & Wong (1996). However, the star has a small protrusion pointing away from Trapezium, which may indicate a propolyd tail. This propolyd tail is very short, suggesting that the object it is highly inclined. A very faint and diffuse arc can be discerned in front of the object, but it is superimposed on an irregular background, which makes it difficult to delineate its form.

066-652. This is in the distant south of the nebula and is so faint that it is impossible to tell whether the nebulosity associated with the star is a stationary arc or instead a bright-rimmed globule.

083-435. The central source shows a very faint tail suggesting that this source is a previously uncatalogued propolyd. There is slight evidence for a broad diffuse emission arc in front of the propolyd, but the source is near to the "SW Cloud" foreground extinction feature (O'Dell & Yusef-Zadeh 2000), and the presence of faint extinction filaments complicates the identification.

117-421. This small propolyd (Ricci et al. 2008) appears to excavate a small cavity around it, but no shell outer edge is evident. Additionally, as for 083-435, the proximity to foreground extinction filaments may be a confusing factor.

121-434. Another small propolyd in the same area, with the appearance of a clump emission arc in front of it. However, once again, the highly variable extinction makes the identification uncertain.

124-131. This object is a circumbinary propolyd, that was first catalogued by O'Dell & Wong (1996), but they named it 124-132 and classified as irregular. Later, this source was reported by Smith et al. (2005) showing a microjet emerging perpendicular to the major axis of the disk. Ricci et al. (2008) cataloged the source as a binary system and Roberto et al. (2008) interpreted the central dark silhouette as a circumbinary disk. We report the discovery of a broad, faint partial shell in front of the propolyd, which we identify as a stationary arc. The arc is barely visible in H α , but is much clearer in green and blue wideband filters, suggesting that we are seeing dust-scattered continuum. In this respect it is similar to the arc in front of the close-in propolyd 163-317 (LV 3).

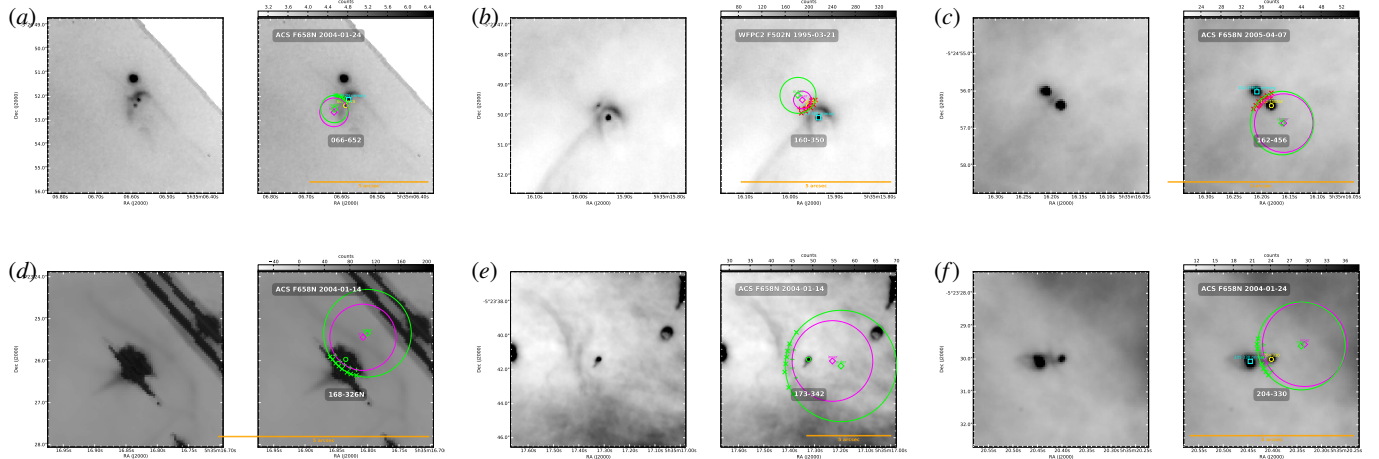
131-046. There is the appearance of a very broad and flat shell in front of this propolyd. However, it is in a region that is Cross-crossed by multiple extinction filaments and the apparent shell may be an illusion.

173-236. This large propolyd is has the weak evidence for an emission arc in front of it, but it has a very small radius of curvature compared with the other arcs. It is located near to the "Dark Bay" (O'Dell & Yusef-Zadeh 2000) and is crossed by multiple extinction filaments, which make the identification uncertain.

212-400. A small propolyd with weak evidence for an emission arc in front of it. As with 173-236, it is near to the

Table 9. Shell geometric parameters of interproplyd shells

| Object | RA | Dec | D | PA | R_{out} | R_{in} | Π_{out} | Π_{in} | Λ_{out} | Λ_{in} | h | PA_{out} | PA_{in} | Star ID |
|----------|-------------|-------------|--------|-------|------------------|-----------------|--------------------|-------------------|------------------------|-----------------------|------|--------------------------|-------------------------|----------|
| 066-652 | 05:35:06.59 | -05:26:52.4 | 255.85 | 34.9 | 0.03 | -0.07 | | | | | 0.10 | 316.8 | 341.9 | ACS 2793 |
| 160-350 | 05:35:15.96 | -05:23:49.7 | 27.91 | 13.3 | 0.11 | 0.04 | | | | | 0.07 | 226.2 | 224.3 | ACS 4341 |
| 162-456 | 05:35:16.18 | -05:24:56.4 | 93.91 | 1.9 | 0.29 | 0.21 | | | | | 0.09 | 28.8 | 49.2 | ACS 4351 |
| 168-326N | 05:35:16.83 | -05:23:26.0 | 7.49 | 297.4 | 0.23 | 0.12 | 5.82 | 6.26 | | 3.36 | 0.11 | 137.0 | 142.2 | ACS 4567 |
| 173-342 | 05:35:17.32 | -05:23:41.4 | 23.46 | 323.5 | 1.29 | 0.83 | 2.95 | 2.46 | | | 0.46 | 82.2 | 76.1 | ACS 4671 |
| 204-330 | 05:35:20.40 | -05:23:30.0 | 60.39 | 277.1 | 0.33 | 0.11 | 3.87 | 7.42 | | 2.01 | 0.22 | 112.4 | 119.0 | ACS 5475 |

**Figure 16.** Stationary arc sources in the Interproplyd shells.

“Dark Bay” and the apparent arc may be an illusion caused by inhomogeneous foreground extinction.

244-440. Giant proplyd. Seems to be in a cavity with a well-defined inner border. But it is not concave around the proplyd. May be a larger scale feature related to the Bright Bar or to HH 203/204.

266-500 (approx). Proplyd. Evidence for small concave arc. This might go in a new group of th1A objects.

095-800 (approx). Very bright star with reflection nebula and comet-shaped arc.

4. DISCUSSION

Proplyd over star fraction falls off relatively smoothly with projected distance. Albeit with a sudden drop after about 200 arcsec.

Bowshock over proplyd fraction seems to have three separate peaks. Very small distances corresponding to the wind-wind interaction, then there is a dearth of bowshocks until a second peak around four arcmin. Finally at very large radii there may be a third peak of objects that are not proplyds.

But an alternate explanation for the third peak could be that they are all proplyds but that the proplyd fraction is underestimated at large distances.

On the other hand there is also evidence for three distinct populations from the azimuthal distribution around the Trapezium. The group at 4 arcmin separation are mainly to the west whereas the more distant objects are mainly to the south.

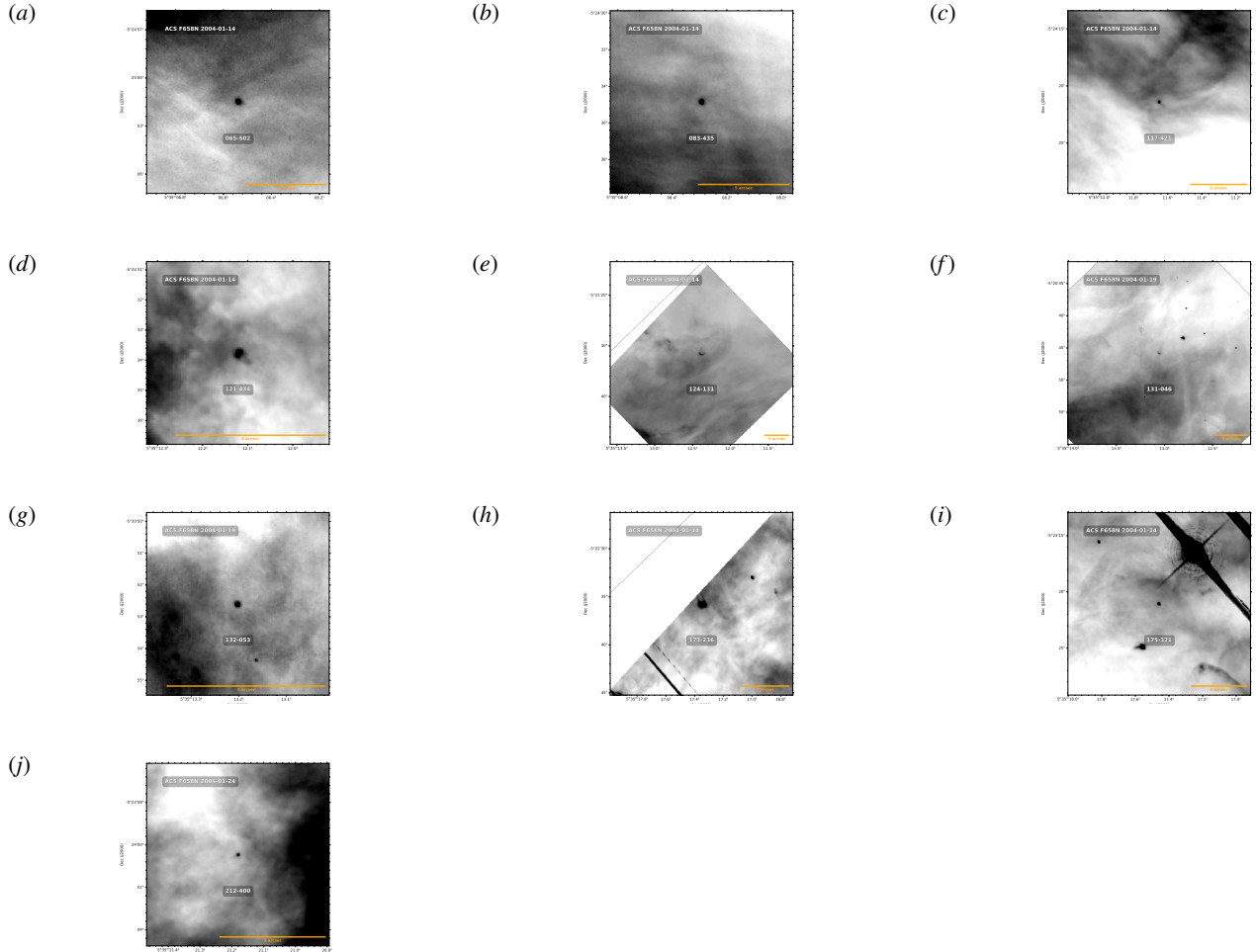
For clarity, we have omitted many secondary features and slightly increased the size of the smaller features, such as Orion South. The sizes of the smaller features of the different features have been modified slightly

REFERENCES

- Bally, J., Licht, D., Smith, N., & Walawender, J. 2006, AJ, 131, 473
- Bally, J., O’Dell, C. R., & McCaughean, M. J. 2000, AJ, 119, 2919
- Bally, J., & Reipurth, B. 2001, ApJ, 546, 299
- . 2018, Research Notes of the American Astronomical Society, 2,

Table 10. Shell geometric parameters of problematic objects

| Object | RA | Dec | <i>D</i> | PA | R_{out} | R_{in} | Π_{out} | Π_{in} | Δ_{out} | Δ_{in} | h | PA_{out} | PA_{in} | Star ID |
|---------|-------------|-------------|----------|-------|------------------|-----------------|--------------------|-------------------|-----------------------|----------------------|------|--------------------------|-------------------------|----------|
| 065-502 | 05:35:06.54 | -05:25:01.5 | 177.29 | 56.1 | 1.42 | 0.49 | 5.13 | | 3.33 | | 1.21 | 90.5 | 104.7 | ACS 2783 |
| 083-435 | 05:35:08.29 | -05:24:34.9 | 140.89 | 59.1 | 1.25 | 0.54 | 1.16 | | 1.55 | | 0.58 | 84.0 | 40.5 | ACS 2951 |
| 117-421 | 05:35:11.65 | -05:24:21.4 | 92.07 | 50.2 | 2.00 | 0.71 | 3.69 | 1.94 | 2.25 | 4.42 | 1.37 | 99.1 | 96.7 | ACS 3388 |
| 121-434 | 05:35:12.12 | -05:24:33.8 | 95.58 | 41.8 | 0.76 | 0.34 | 1.93 | 2.75 | | 1.96 | 0.39 | 65.4 | 66.2 | ACS 3463 |
| 124-131 | 05:35:12.38 | -05:21:31.4 | 126.20 | 151.7 | 4.48 | 2.74 | | | | | 1.73 | 134.9 | 156.0 | ACS 3497 |
| 131-046 | 05:35:13.06 | -05:20:45.8 | 164.46 | 162.4 | 3.55 | 1.00 | 2.04 | 9.64 | | | 2.17 | 140.3 | 144.2 | ACS 3586 |
| 132-053 | 05:35:13.20 | -05:20:52.6 | 157.31 | 162.4 | 0.72 | 0.32 | 4.77 | 1.57 | 1.57 | 2.60 | 0.39 | 153.9 | 167.0 | ACS 3618 |
| 173-236 | 05:35:17.35 | -05:22:35.7 | 48.96 | 197.1 | 2.28 | 1.53 | | | | | 0.75 | 255.3 | 275.5 | ACS 4705 |
| 175-321 | 05:35:17.46 | -05:23:21.1 | 16.03 | 264.7 | 2.03 | 1.38 | | 1.79 | | | 0.60 | 298.7 | 324.5 | ACS 4719 |
| 212-400 | 05:35:21.18 | -05:24:00.5 | 80.99 | 297.9 | 1.07 | 0.84 | | | | | 0.21 | 331.2 | 335.5 | ACS 5617 |

**Figure 17.** Stationary arc sources in the Problematic objects.

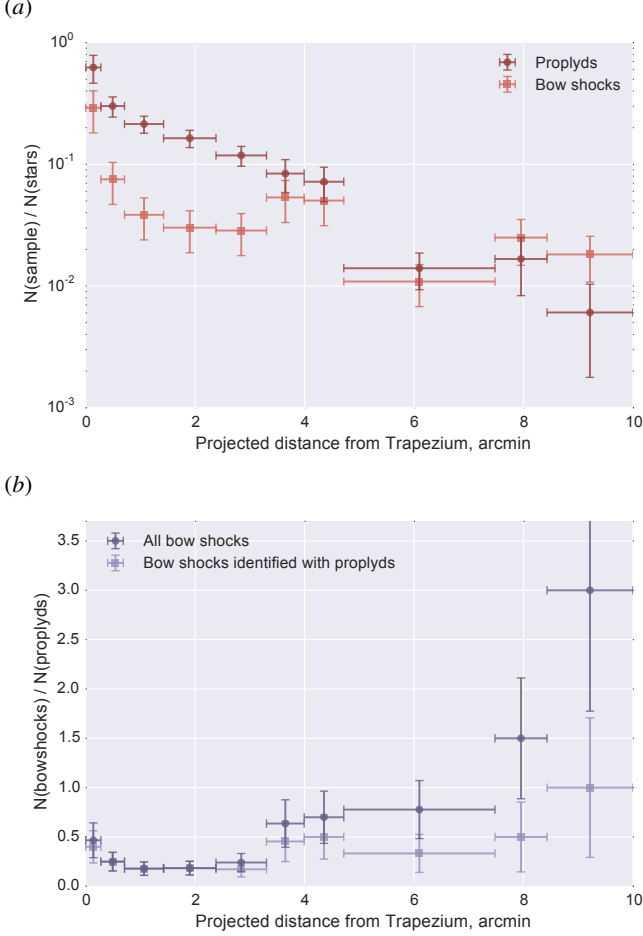


Figure 18. (a) Fraction of all optically visible stars that are proplyds (dark circle symbols) or have bowshocks (light square symbols) as a function of projected separation from the Trapezium. (b) Ratio between number of bowshocks and number of proplyds as a function of projected separation from the Trapezium. Dark circle symbols show all bowshocks in our catalog (with the exception of interproplyd shocks) while light square symbols show only those bowshocks associated with known or suspected proplyds.

- Bally, J., Sutherland, R. S., Devine, D., & Johnstone, D. 1998, AJ, 116, 293
 Da Rio, N., Robberto, M., Soderblom, D. R., Panagia, N.,
 Hillenbrand, L. A., Palla, F., & Stassun, K. 2009, ApJS, 183, 261
 Graham, M. F., Meaburn, J., Garrington, S. T., O'Brien, T. J.,
 Henney, W. J., & O'Dell, C. R. 2002, ApJ, 570, 222
 Gull, T. R., & Sofia, S. 1979, ApJ, 230, 782
 Henney, W. J., García-Díaz, M. T., O'Dell, C. R., & Rubin, R. H.
 2013, MNRAS, 428, 691
 Hillenbrand, L. A. 1997, AJ, 113, 1733
 Laques, P., & Vidal, J. L. 1979, A&A, 73, 97
 O'Dell, C. R., & Wen, Z. 1994, ApJ, 436, 194
 O'Dell, C. R., & Wong, K. 1996, AJ, 111, 846
 O'Dell, C. R., & Yusef-Zadeh, F. 2000, AJ, 120, 382

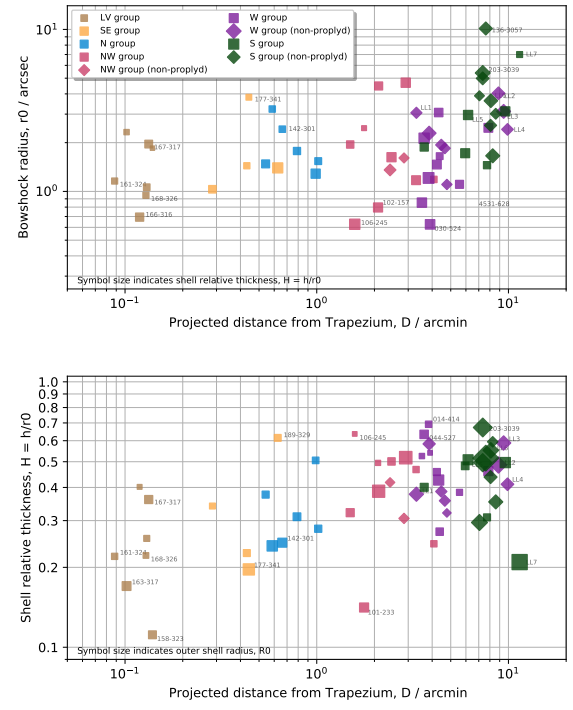


Figure 19. Bowshock axial size (panel a) and relative thickness (panel b) versus distance from the Trapezium.

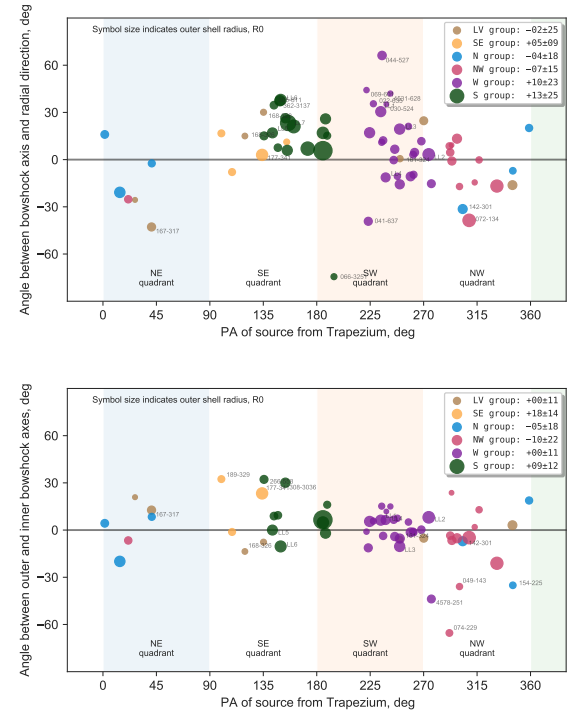


Figure 20. Angle offset between bowshock axis and the radial direction to θ^1 Ori C.

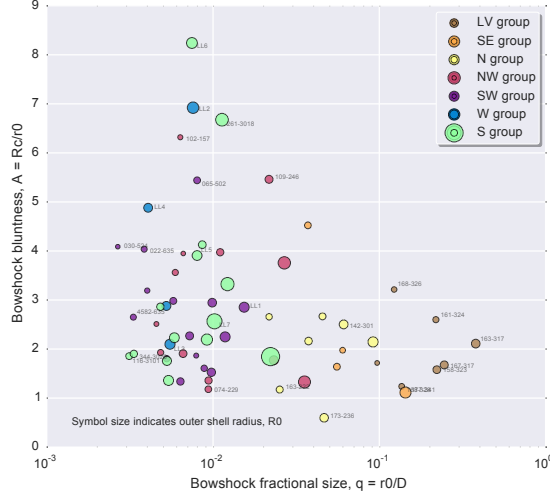


Figure 21. Bowshock bluntness versus relative size.

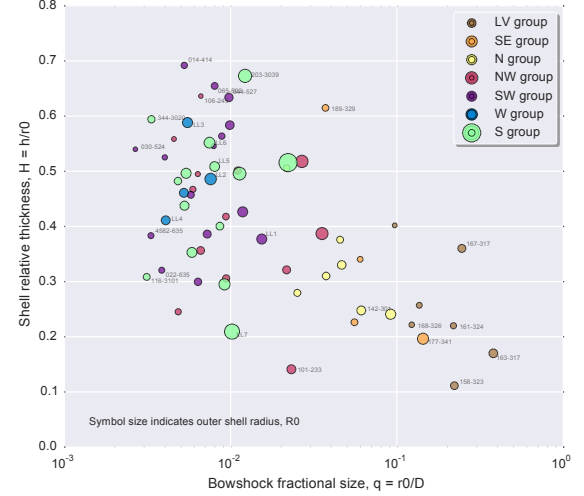


Figure 22. Bowshock relative shell thickness versus relative size.

- Parihar, P., Messina, S., Distefano, E., Shantikumar, N. S., & Medhi, B. J. 2009, MNRAS, 400, 603
 Reipurth, B., Guimarães, M. M., Connelley, M. S., & Bally, J. 2007, AJ, 134, 2272
 Ricci, L., Roberto, M., & Soderblom, D. R. 2008, AJ, 136, 2136
 Roberto, M., Ricci, L., Da Rio, N., & Soderblom, D. R. 2008, ApJL, 687, L83
 Roberto, M., et al. 2013, ApJS, 207, 10
 Smith, N., Bally, J., Shuping, R. Y., Morris, M., & Kassis, M. 2005, AJ, 130, 1763

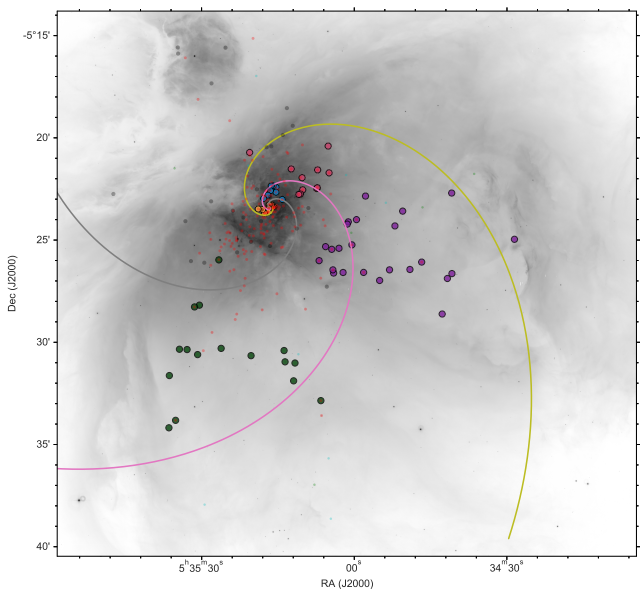


Figure 23. The interlocking spirals.

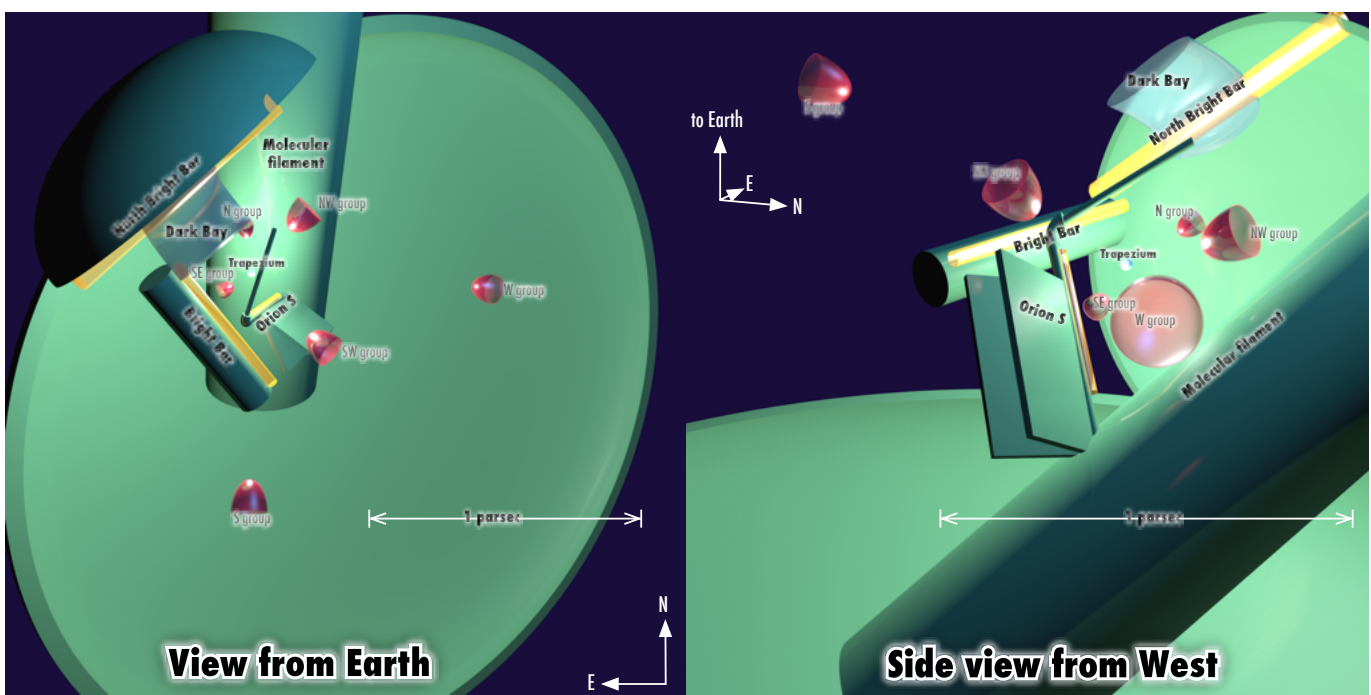


Figure 24. Simplified three-dimensional structure of the Orion Nebula.